PC

Notes for lectures on dynamics

T N Palmer

Contents

INTERNATIONAL ATOMIC ENERGY AGENCY
UNITED NATIONS EDUCATIONAL, SCIENTIFIC AND CULTURAL ORGANIZATION

INTERNATIONAL CENTRE FOR THEORETICAL PHYSICS
34100 TRIESTE (ITALY) - P.O.B. 586 - MIRAMARE - STRADA COSTIERA 11 - TELEPHONES: 224281/2/3/4/5/6
CABLE: CENTRATOM - TELEX 460392-1

SMR/113 - 19

AUTUMN COLLEGE

ON

THE TROPOSPHERE, STRATOSPHERE AND MESOSPHERE

10 September - 19 October 1984

NOTES FOR LECTURES ON DYNAMICS

T.N. PALMER

Meteorological Office
London Road
Bracknell, Berkshire RG12 2SZ
U.K.

INTRODUCTION

A study of the mechanics of wave-like motions in the atmosphere can be divided in two parts, kinematics and dynamics. Kinematics can be thought of as the format in which you input and output information about the system under investigation, to and from the dynamics, the latter being a kind of 'central processor'.

A kinematical specification is important. It can make the difference between

1) mathematical analysis being easy or intractable
2) observational diagnostics being straightforward or impossible to calculate
3) physical interpretation being obvious or obscure.

Unfortunately 1), 2) and 3) are not always compatible.

Since the earth's rotation plays an important role in the dynamics of large scale atmospheric waves, one kinematical specification of an atmospheric fluid variable ψ is to write it as the sum of a zonal mean and a deviation from the zonal mean

$$\psi(z,\phi,\lambda) = \bar{\psi}(z,\phi) + \psi'(z,\phi,\lambda)$$

where $\bar{\psi}$ is the Eulerian mean of ψ round the latitude circle ϕ = constant, λ being longitude, z height above the earth's surface.

In analytical models, it is often assumed that ψ' is a small perturbation, ie

$$\psi' = O(\epsilon)\,\bar{\psi} \quad , \quad \epsilon \ll 1$$

We call the primed variables, eddies.

To $O(\epsilon)$ the dynamics are linearised, and the Eulerian mean kinematical description takes the form

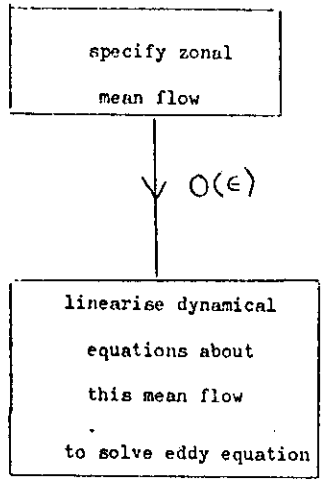

Waves are created (eg by instability) or modified (eg from wave-like forcing at a boundary) by the specified mean flow.

Since terms like $\overline{\psi'^2} \neq 0$, then to $O(\epsilon^2)$, the waves react back on the mean flow, ie

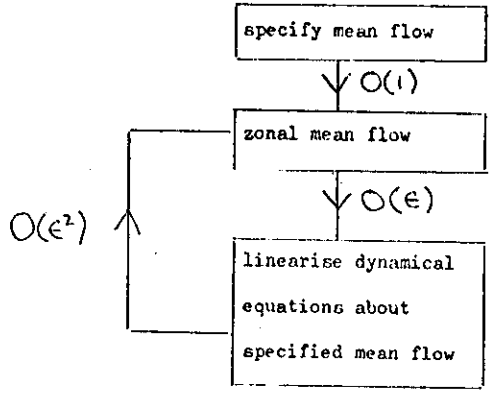

For finite amplitude waves (all wave amplitudes are finite in practice) we have a continuous feedback system, comprising the problem of

wave, mean-flow interaction
(i) How the waves change the mean flow
(ii) How mean-flow profiles react back on the waves.

Whether (i) comes before (ii) or vice-versa is really a chicken-and-egg argument.

In these lectures I hope to show that

a) Wave mean-flow interaction is important in the atmosphere, and can result in some rather surprising fluid motions.

b) Blind use of the Eulerian mean kinematic description in rotating fluids can lead to results which are difficult to interpret physically, and only until recently have caused some confusion in the literature.

In order to convince you of points a) and b), I shall consider rather simple examples - the internal gravity wave, and the inertio-gravity wave. These waves illustrate the essentials of wave, mean-flow interaction occurring in the more complex atmospheric wave motions.

Internal gravity waves

We consider 2-dimensional steady, adiabatic buoyancy waves generated by a slippery boundary moving parallel to itself with constant velocity c (= phase speed of waves). Assume initial 'zonal' velocity (spacial average along Z = constant) is zero.

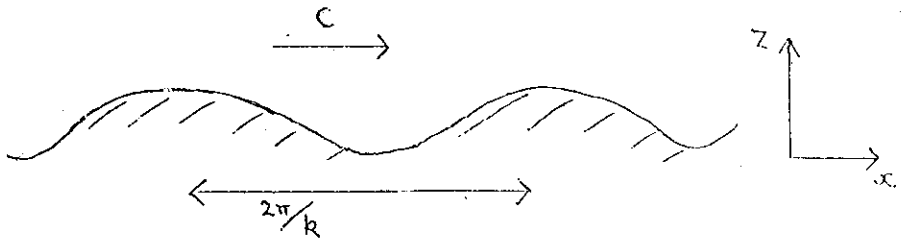

In order that buoyancy waves are generated and propagate upwards, the forcing frequency $\omega = ck$ must satisfy

$$0 < \omega \leq N$$

where N is the Brunt-Vaisala frequency. These inequalities can be derived from the dispersion relation of the eddy wave equation, but can be seen by considering the analogy of a pendulum with natural frequency N, being forced by your hand (say) oscillating with frequency ω. If $\omega = 0$ nothing happens; if $\omega = N$ the bob oscillates at the natural frequency of the pendulum; if $\omega > N$ you destroy the oscillatory motion of the bob. So with the particles of the fluid. Note that if the initial zonal velocity of the fluid, $\bar{u}$, $\neq 0$ then the condition for no wave forcing is

$$\omega_{\text{DOPPLER}} \equiv (c - \bar{u})k = 0$$

With a little thought, we can draw the eddy velocities of the fluid particles as they respond to wave forcing and buoyancy forces

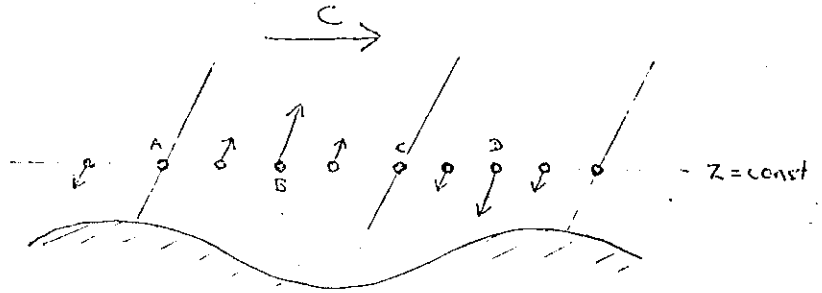

Particle A is at the top of its oscillation

Particle B is at the mid-point of its oscillation travelling up

Particle C is at the bottom of its oscillation

Particle D is at the mid-point of its oscillation travelling down.

hence

The temperature perturbation at A is negative (adiabatic ascent)

" " " " B is zero (neutral point)

" " " " C is positive (adiabatic subsidence)

" " " " D is zero (neutral point)

Note from the diagram that the zonal mean temperature perturbation is zero. The general temperature and pressure perturbation structure for the steady wave can easily be deduced

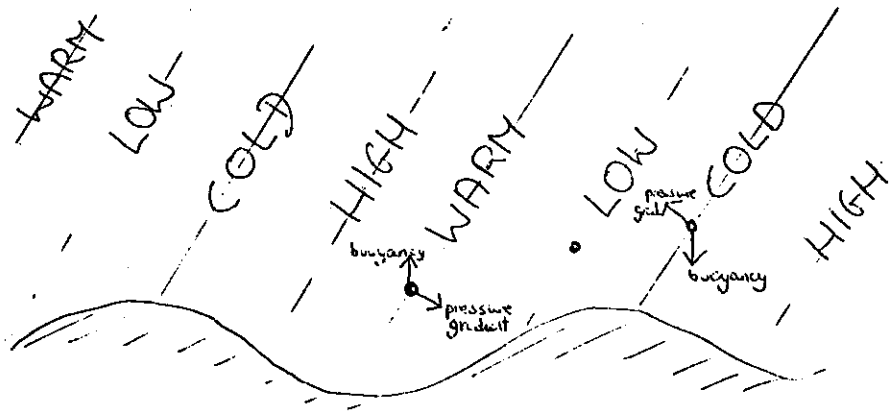

The smaller the (Doppler) frequency of wave forcing, the flatter the particle oscillations and the temperature and pressure phase lines.

Another result we shall need concerns the eddy velocity $\underline{u}' = (u', w')$. Note that u' is positively correlated with w' ie when $u' > 0$, $w' > 0$, and when $u' < 0$, $w' < 0$, so that $\overline{u'w'} > 0$

In a region of steady wave forcing with no wave dissipation, the eddy velocities increase as the fluid gets more rarified, keeping the upward flux of eddy momentum $\rho\overline{u'w'}$ constant with height. (Here, of course,

ρ is the zonal mean density of the fluid). Put another way; in the absence of wave transience and dissipation

$$\frac{\partial}{\partial z}\left(\rho\overline{u'w'}\right) = 0$$

If the waves are dissipating, then the eddy momentum flux will decrease with height. Where does this momentum go? It goes into accelerating the zonal mean flow. This information is contained in the zonal mean momentum equation

$$\frac{\partial \bar{u}}{\partial t} = -\frac{1}{\rho}\frac{\partial}{\partial z}\left(\rho\overline{u'w'}\right) + \bar{X}$$

where $\bar{X}$ is a mean dissipative term. Note also that at the leading wave front, eddy momentum is injected into the mean flow, causing mean flow acceleration. We ascribe such a situation to wave transience. We could of course have obtained all the preceding information from the wave equation and resulting dispersion relation. Here I wish to emphasis what the particles are doing. The reason for this will become apparent in the next lecture.

Let us suppose some dissipation is present in the steady waves, and represent a 'dissipative height scale' by D, i.e., eddy momentum fluxes decrease as exp (-z/D). It turns out that the more horizontal particle oscillations are, the smaller will be the dissipative height scale. (To show this rigorously we would need to discuss the so-called conservation of wave-action equation, and the associated group velocity of the waves.)

Let us examine the complete wave, mean-flow interaction for this system. The dissipating wave will induce a mean-flow acceleration throughout a depth D. But now the Doppler-shifted frequency of the wave becomes less than it was before the mean-flow acceleration. Hence the particles oscillate in slightly more horizontally tilted lines.

Therefore the scale height D decreases, and further mean-flow acceleration occurs throughout a smaller depth. This feedback process continues, and a sizeable mean flow will develop near the bottom of the fluid. Eventually the mean flow velocity becomes equal to the velocity of the slippery corrugated boundary, ie the Doppler shifted frequency of the waves becomes equal to zero, and as we have seen, when this happens, the waves can no longer propagate up - we have reached impasse! Pictorially the mean-flow evolves as

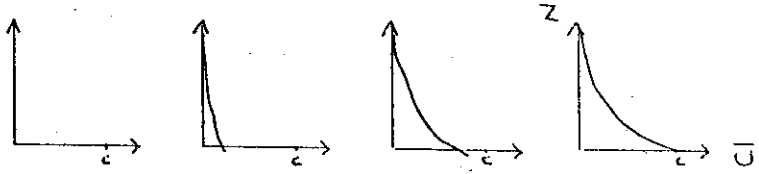

We have assumed that mean-flow dissipation is unimportant.

If we now add to the input of waves at $Z = 0$, a component travelling with equal and opposite phase speed $-C$, something very interesting happens. If the two waves, with phase speeds $\pm C$, have equal amplitudes, then the boundary executes a standing wave

$$Z = a \sin k(x-ct) + a \sin k(x+ct)$$
$$= 2a \sin kx \cos kct$$

Now, as we have seen, the wave travelling in the positive x direction cannot propagate up, but the one travelling in the negative x direction can (providing its Doppler shifted frequency $2kc$ is less than N). Hence, this wave starts to accelerate the mean flow in the negative x direction. Because its Doppler shifted frequency is comparatively large, a negative mean acceleration is induced throughout a comparatively deep layer,

leading to the appearance of a downward moving zero in the mean velocity profile, as illustrated below.

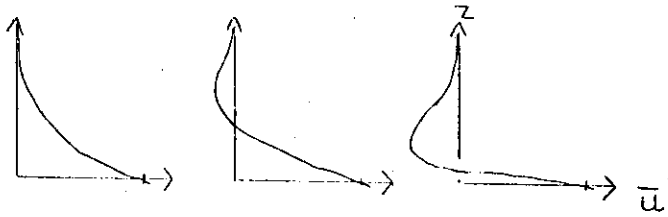

When the shear gets large at the bottom of the fluid, the Richardson number gets small, and the shear layer goes turbulent.
The final velocity profile is, therefore

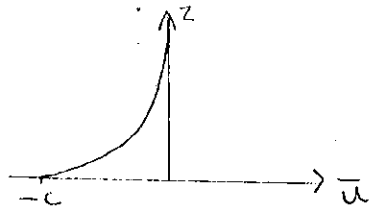

Suppose we start with no zonal flow, and switch on a standing wave at the bottom. What happens? If viscosity is not too great, then an instability occurs, and a vacillation in the mean-flow results with the zero of the mean velocity propagating down. Figure 1 should explain this instability.

That such phenomena occur in real fluids has recently been most beautifully demonstrated in the laboratory by Plumb and McEwan (Plumb, R.A. and A.D. McEwan (1978) J. Atmos. Sci. 35, 1827-1839). The meteorological relevance of this wave, mean-flow interaction, is that

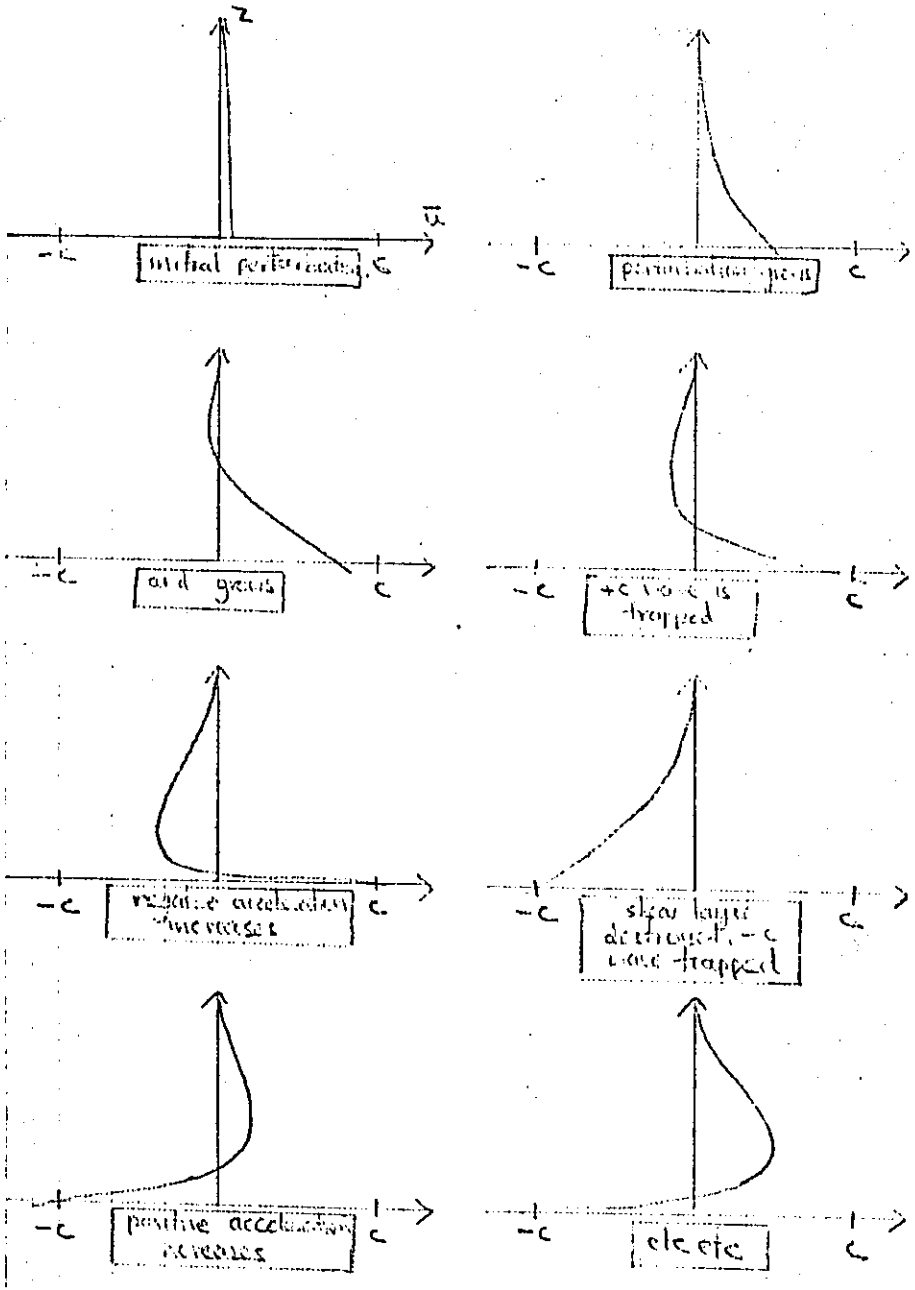

FIG 1

it demonstrates in the laboratory, an analogue of the stratospheric quasi-biennial oscillation (for more details of this, see the course on the stratosphere). Plumb and McEwan's film of the simulated QBO beautifully demonstrates wave, mean-flow interaction! Who would have thought that downward propagating easterlies, then westerlies, then easterlies was due to the input of a steady standing wave from below?

Inertia-gravity waves

Let us now consider steady buoyancy waves with the added complication of rotation. Again I shall be rather descriptive, and not bother too much with mathematical analysis. We shall find that the Eulerian-mean description of these waves is somewhat misleading, and this has led to the recent formulation of a "Lagrangian-mean" description of such motions. Such a description of fluid motions has proved useful in the stratosphere, both in understanding its dynamical behaviour, and in understanding how passive chemical tracers are transported.

We consider the idealisation of an inviscid diffusionless fluid of constant buoyancy frequency N, rotating about the z-axis with constant angular velocity $\Omega = \frac{1}{2} f$. The fluid is contained in a channel, between rigid vertical walls at $y = 0, b$ and a moving lower boundary $z = h(x,y,t)$ with, as before, $\bar{h} = 0$.

Let's also suppose the forcing from below has maximum amplitude at mid-channel

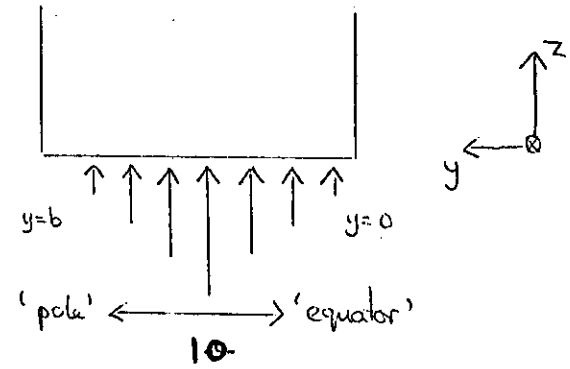

If the wave forcing has phase speed -C (in the x direction), we can draw the particle oscillations in the x-z plane from our knowlege of buoyancy waves

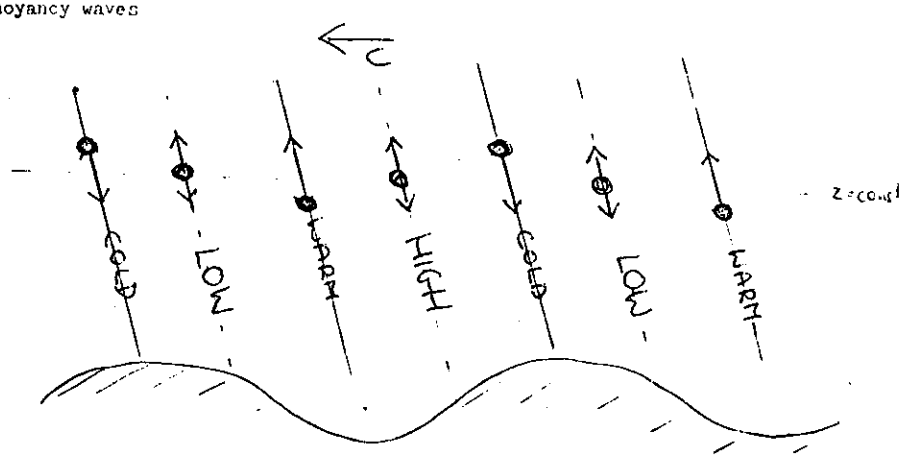

The particles however also oscillate in the 'meridional' direction because of Coriolis forces. Let us determine the meridional velocity (qualitatively at least), from the geostrophic relationship

$$v' = \frac{1}{f\rho}\frac{\partial p'}{\partial x}$$

From this relationship, we can see that

when $u'=0$ (at top of oscillation), $\partial p'/\partial x < 0$, $v'<0$

when $u'<0$ (at mid-point, going down), $\partial p'/\partial x = 0$, $v'=0$

when $u'=0$ (at bottom of oscillation), $\partial p'/\partial x > 0$, $v'>0$

when $u'>0$ (at mid-point, going up), $\partial p'/\partial x = 0$, $v'=0$

Putting all this information together we see that the particles paths are spirals (if viewed from a frame in which the forcing is stationary)

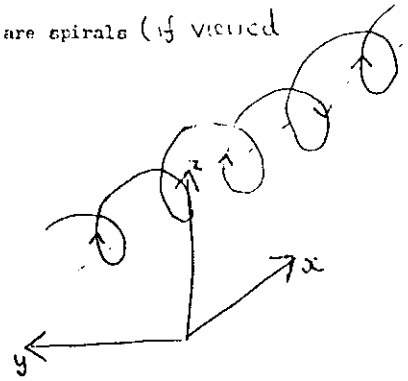

Projecting onto the y, z plane (the 'meridional plane'), the paths are ellipses

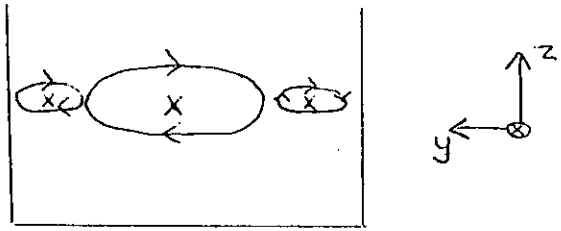

whose sizes are related to the amplitude of wave forcing. When the waves are steady, then clearly the average position of the particles, marked by Xs, does not change with time. (Note that since the particles have meridional components of velocity, Coriolis forces are also felt in the x-direction. This means that particle oscillations in the x-z plane are more horizontal than they would be if there was no rotation.

In other words, rotation tends to supress the upward propagation of buoyancy waves. It turns out that when $\omega = f$, the waves are completely suppressed).

Assuming that $f < \omega < N$, what picture does the Eulerian mean formalism present for these steady waves? Consider first an ellipse whose centre is at the 'latitude' of maximum forcing

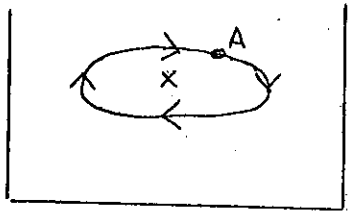

At the top of the ellipse $v' < 0$, but so also is T', $\therefore v'T' > 0$. At the bottom of the ellipse $v' > 0$, so also is T', $\therefore v'T' > 0$, ie v' is positively correlated with T' throughout the particle oscillation. If we take an arbitrary point A on the ellipse, then the zonal mean of $v'T'$ at A must also be positive, ie $\overline{v'T'} > 0$. Since A is arbitrary, $\overline{v'T'} > 0$ everywhere.

Hence we have a somewhat paradoxical picture of an eddy heat flux which is directed towards $y = 0$ ('poleward') everywhere, even though there is no net heat transport towards the pole (because, on average, particles are not going anywhere). In other words, even though the eddy heat flux is poleward, the pole is not being heated! Note the fact that $\overline{v'T'} > 0$ is independent of whether there exists a positive or negative zonal mean temperature gradient between y = b and y = 0. Hence, any attempt to parametrize the eddies with a diffusive type parameter

$$\overline{v'T'} = \kappa \frac{\partial \bar{T}}{\partial y}$$

is doomed to failure. The heat flux is related to the wave forcing not to the mean temperature gradient.

If the wave forcing had positive phase speed then it can easily be shown that $\overline{v'T'}$ would be negative everywhere, implying an 'equatorward' heat flux. Since particle trajectories are parallel to lines of constant phase ($\underline{u}' = \mathrm{Re}\{\underline{A} e^{i\phi}\} \Rightarrow \mathrm{div}\,\underline{u}' = \underline{u}' \cdot \nabla\phi = 0$ (incompressibility) $\Rightarrow \underline{u}' \perp \nabla\phi = \text{const}$), we have derived the well-known relation that the phase lines must tilt west with height to get poleward heat fluxes.

What is the resolution of this paradox? Consider the two ellipses

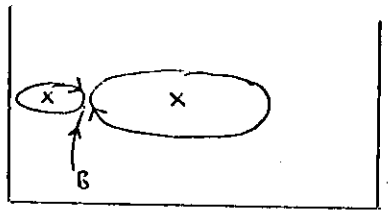

At the point B, the particle of the large ellipse is moving upward, the particle of the small ellipse is moving downward. The net result is an upward velocity (the larger the amplitude, the larger the velocity). Hence the Eulerian mean vertical velocity at B is positive. In fact at any point 'north' of the centre of the ellipse at maximum forcing, the Eulerian mean vertical velocity is positive. Conversely, at any point 'south' of the centre of the ellipse, the Eulerian mean vertical velocity is negative.

Hence, the full Eulerian mean picture can be summarised by the following diagram

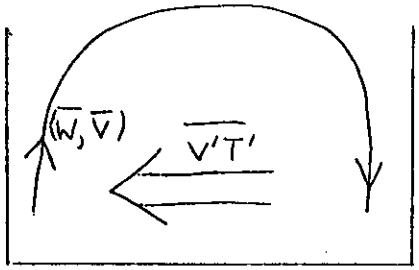

The eddy heat flux induces a mean meridional circulation. Adiabatic ascent over the pole balances the eddy heat flux input, and adiabatic subsidence over 'low-latitudes' balances the eddy heat flux output. The whole system organises itself so that no net heat or momentum is transferred to the mean-flow.

This result, that when waves are steady the zonal flow is not acclerated or heated, has the status of a theorem in the literature, the so-called Charney-Drazin theorem (Charney, J.G., and P.G. Drazin 1961, J. Geophys. Res. 66 83-109) and indeed it is a difficult result to prove in an Eulerian-mean kinematic description. Nevertheless we have seen that for steady, non-dissipative waves, the fluid particles do not on average get anywhere - a very straightforward physical result. Surely there must be some kinematic description in which the Charney-Drazin theorem is immediate? Indeed there is - it is the 'Lagrangian mean' description; Lagrangian because the averaging is related to particle trajectories, as opposed to Eulerian where the averaging is related to Eulerian where the averaging is related to fixed points in space.

Before describing a little of the kinematic formulation of Lagrangian mean theory, it is worth spending a little time discussing the meteorological relevance of the above considerations.

Dynamic processes in the stratosphere result not from in situ instabilities, but rather from tropospheric forcing. Of particular interest are the mid-latitude tropospheric planetary waves. Occasionally, the amplitudes of these waves reach rather high values - we refer to the meteorological condition when this happens by the adjective blocking. If conditions are right (which only happens in the winter), these high amplitude waves propagate up into the stratosphere. As the leading wave front moves up, the manifestly transient conditions decelerate the westerly zonal mean flow. The effects of this deceleration are felt most keenly at high altitudes and high latitudes, firstly because air is rather tenuous at high altitudes, and secondly the mass of air between two neighbouring latitude circles decreases with latitude. Because the zonal flow is decelerated at the leading wave front, it is no longer in geostrophic balance, and air flows into the low pressure region over the stratospheric pole. The result is a Lagrangian meridional circulation with descending air over the stratospheric pole. By adiabatic subsidence, the stratospheric pole heats up very dramatically - sometimes by 40° in just a few days. The Lagrangian meridional circulation is illustrated below

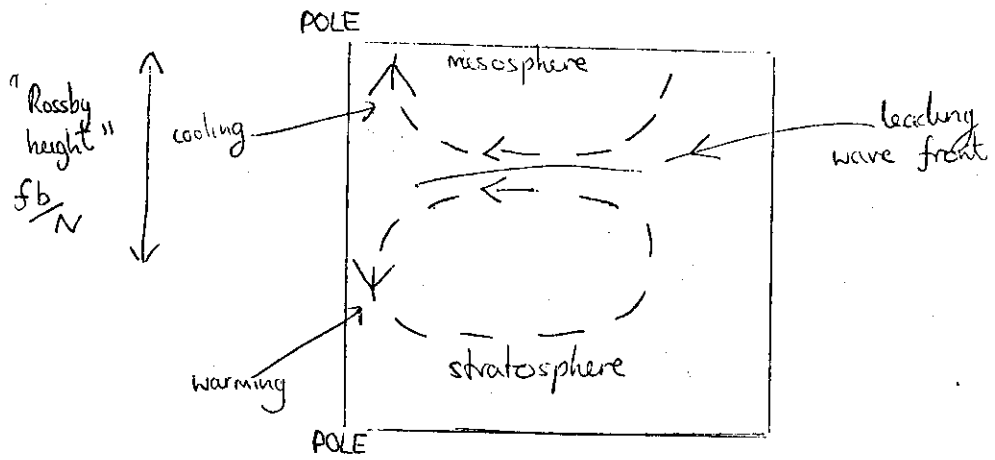

The magnitude of this Lagrangian circulation has been quantified by Matsuno and Nakumara (Matsuno T. and K. Nakaraira K. 1979, J. Atmos. Sci. 36, 640-654). The Lagrangian picture gives a rather straightforward explanation of this phenomenon, named, rather appropriately, the stratospheric sudden warming. By contrast, the Eulerian mean description replete with its ficticious eddy heat fluxes and mean meridional circulations, gives a rather complicated explanation of the sudden warming - certainly one would have little idea that the warming was due to mass subsidence. Consequently much of the literature on the subject is rather obscure as far as providing an understanding of the physical mechanisms of a warming.

Lagrangian-mean kinematics

The Lagrangian-mean theory, recently developed (Andrews D.G. and M.E. McIntyre 1978 J. Fluid. Mech. 89, 609-646) is a hybrid kinematic description, lying somewhere between Stokes classical idea of taking the time mean following a single air parcel, and the Eulerian mean description of taking means with respect to fixed latitude circles.

Consider a number of fluid particles lying along a latitude circle at an initial time t_0, before the wave forcing has begun. When the wave propagates up the particles are displaced. Imagine the particles are attached by elastic bands to a 'magic' rod of zero mass which is constrained, for all time, to be parallel to latitude circles. Initially the particles sit on the rod. When the particles are displaced, the rod is moved by the tension in the elastic bands, from its initial latitude circle, to another one. This is illustrated below

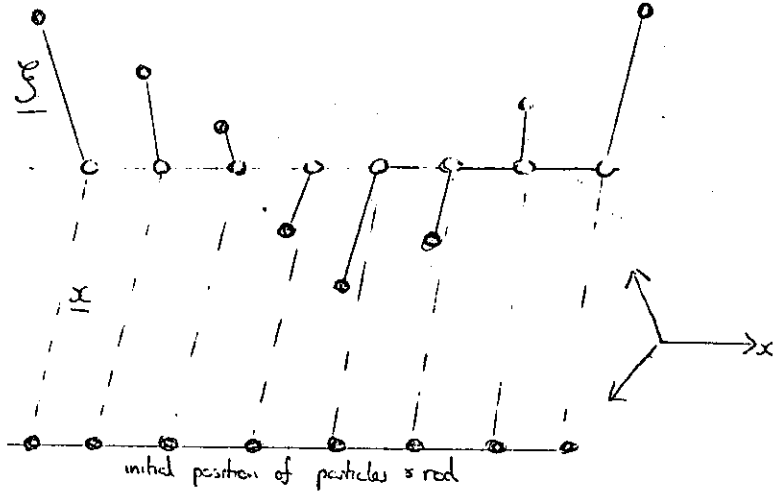

The position vector of the particles, $\underline{\xi}$, relative to the magic rod satisfies $\overline{\underline{\xi}} = 0$ for all time. The position vector of the points of attachment of the elastic bands to the rod, relative to their initial positions, is written as $\underline{x}$. The Lagrangian-mean of some property ψ of the fluid is defined by

$$\overline{\psi(\underline{x},t)}^{L} = \overline{\psi(\underline{x}+\underline{\xi}(\underline{x},t),t)}$$

i.e. each point of attachment assumes the value ψ of its associated particle, and the Lagrangian-mean is the zonal mean along the 'magic' rod. The Lagrangian-mean velocity of the fluid is defined to be the velocity of the points of attachment.

I have deliberately stripped this description of its mathematics; if you are concerned that the formalism lacks rigour, I recommend you look up the Andrews and McIntyre reference. (*)

As an example of the conceptual simplicity of the Lagrangian mean kinematical description, the Lagrangian mean potential temperature, θ, in an adiabatic atmosphere, satisfies

$$\left(\frac{\partial}{\partial t} + \bar{v}^L \frac{\partial}{\partial y} + \bar{w}^L \frac{\partial}{\partial z}\right) \bar{\theta}^L = 0$$

Compare this with the Eulerian mean equation

$$\left(\frac{\partial}{\partial t} + \bar{v}\frac{\partial}{\partial y} + \bar{w}\frac{\partial}{\partial z}\right)\bar{\theta} = -\frac{1}{\cos\phi}\frac{\partial}{\partial y}\left(\overline{v'\theta'}\cos\phi\right) - \frac{1}{\rho}\frac{\partial}{\partial z}\left(\rho\overline{w'\theta'}\right)$$

where ϕ is latitude.

The formalism has successfully been applied to such problems as stratospheric sudden warmings (see above), baroclinic instability* and chemical tracer transport+.

An important and immediate consequence of Lagrangian mean theory is that for steady non-dissipative waves in a zonal mean flow

$$\bar{v}^L = \bar{w}^L = 0$$

This result, as we have seen, is definitely not true of the Eulerian velocities $\bar{v}$, $\bar{w}$. If we write

* Uryu, M., 1979, J. Met. Soc. Japan 57, 1-20.

+ Dunkerton, T., 1978, J. Atmos. Sci., 35, 2325-2333.

$$\bar{v} = \bar{v}^L + \bar{v}^S$$
$$\bar{w} = \bar{w}^L + \bar{w}^S$$

then $(\bar{v}^S, \bar{w}^S)$ is called the "Stokes drift" in the meridional plane. For steady non-dissipative linear waves, the Stokes drift may be written

$$\bar{v}^S = \frac{1}{\rho}\frac{\partial}{\partial z}\left(\rho \overline{v'\theta'}\Big/\frac{\partial\bar{\theta}}{\partial z}\right)$$

$$\bar{w}^S = \frac{1}{\cos\phi}\frac{\partial}{\partial y}\left(\cos\phi\, \overline{v'\theta'}\Big/\frac{\partial\bar{\theta}}{\partial z}\right)$$

Hence, if we define the Eulerian-mean "residual" velocities

$$\bar{v}^* = \bar{v} - \frac{1}{\rho}\frac{\partial}{\partial z}\left(\rho \overline{v'\theta'}\Big/\partial\bar{\theta}/\partial z\right)$$

$$\bar{w}^* = \bar{w} + \frac{1}{\cos\phi}\frac{\partial}{\partial y}\left(\cos\phi\, \overline{v'\theta'}\Big/\partial\bar{\theta}/\partial z\right)$$

then although $(\bar{v}^*, \bar{w}^*)$ are not Lagrangian mean velocities in general they should be closer to them than the Eulerian mean pair $(\bar{v}, \bar{w})$. Since the Lagrangian mean displacement vector is not directly observable from radiosonde or satellite radiance measurements, a kinematic formalism based on these 'residual' velocities should be a nice compromise between the theoretically important Lagrangian mean theory, and the Eulerian mean formalism (which has the advantage of fitting rather straightforwardly into an observational diagnostic scheme).

Indeed wave, mean-flow interactions in the stratosphere have been diagnosed using measurements from the Meteorological Office's Stratospheric Sounding Units, flown on the Tiros-N and Noaa-A satellites, and they have given interesting new insights into the dynamics of the stratosphere during a sudden warming.

and the second order solution becomes the WKBJ solution

$$y(x) = \frac{A}{|f|^{1/2}} e^{\pm i\int |f| dx}$$

The solution fails if f changes too rapidly or if f passes through zero. A convenient form to express the WKBJ solution is in terms of a 'long' space variable $X = \tau x$, $\tau << 1$, over which f is presumed to have O(1) variation. (i.e., $|df/dX| \sim f^2$). In terms of this

$$y(x) = y_o(X) e^{i\Phi(X)/\tau}$$

where $\Phi(X) = \pm\int |f| dX$, $y_o(X) = A/|f|^{1/2}$

Internal Gravity (or Buoyancy) Waves

These waves exist in an atmosphere that is stably stratified so that a fluid parcel displaced vertically will undergo buoyancy oscillations with frequency N (see earlier discussion in the notes). We suppose that the horizontal scale L of these waves is sufficiently small that Ro >> 1 and the equations of motion can be written as

$$\frac{\partial u}{\partial t} + u\frac{\partial u}{\partial x} + w\frac{\partial u}{\partial z} + \frac{1}{\rho}\frac{\partial p}{\partial x} = \delta_x \qquad \text{(i)}$$

$$\frac{\partial w}{\partial t} + u\frac{\partial w}{\partial x} + w\frac{\partial w}{\partial z} + \frac{1}{\rho}\frac{\partial p}{\partial z} + g = \delta_z \qquad \text{(ii)}$$

where, for simplicity we limit our discussion to two-dimensional internal gravity waves propagating in the x-z plane. The terms δ_x, δ_z stand for any additional terms (e.g., acceleration due to viscous forces) that may be present in the momentum equation. We shall also suppose that the vertical scale of the motions is much smaller than a typical scale-height, i.e., D << H, so that the continuity equation can be written as

$$\frac{\partial u}{\partial x} + \frac{\partial w}{\partial z} = 0 \qquad \text{(iii)}$$

Finally, the thermodynamic equation is

$$\frac{\partial \theta}{\partial t} + u\frac{\partial \theta}{\partial x} + w\frac{\partial \theta}{\partial z} = \mu \qquad \text{(iv)}$$

where μ is a diabatic term.

First of all write

$$p = \tilde{p}(z) + \hat{p} \qquad \rho = \tilde{\rho}(z) + \hat{\rho} \qquad \theta = \tilde{\theta}(z) + \hat{\theta}$$

where $\tilde{p}$, $\tilde{\rho}$, $\tilde{\theta}$ are hydrostatic values for a resting atmosphere (note the new notation)

Now in the horizontal momentum equation (1), the pressure gradient must be balanced against the inertial acceleration (Ro >> 1), i.e.,

$$U^2/L \sim \hat{p}/\tilde{\rho}L$$

where U is a measure of u. Hence using the gas law

$$\hat{p}/\tilde{p} \sim Ma^2 \sim 10^{-5} \quad \text{if} \quad U \sim 1 \text{ m s}^{-1}$$

On the other hand, the adiabatic thermodynamic equation will balance if

$$\frac{\hat{\theta}}{\tilde{\theta}}\frac{U}{L} \sim \hat{w}\frac{1}{\tilde{\theta}}\frac{d\tilde{\theta}}{dz}$$

Now from (iii), $\hat{w} \sim U(D/L)$ $\qquad (\partial u/\partial x \sim U/L)$

hence the thermodynamic equation will balance if

$$\frac{\hat{\theta}}{\tilde{\theta}} \sim \frac{D}{\tilde{\theta}}\frac{d\tilde{\theta}}{dz} \sim \frac{DN^2}{g}$$

If D << H then $D \lesssim 10^3$ m. With $N^2 \approx 10^{-4}$ s^{-2}, $D \sim 10^3$ m

$$\hat{\theta}/\tilde{\theta} \sim 10^{-2}$$

Hence

$$\hat{\theta}/\tilde{\theta} >> \hat{p}/\tilde{p}$$

However, from the definition of potential temperature and the ideal gas law

$$\ln \rho = \frac{1}{\gamma}\ln p - \ln \theta + \text{const.} \qquad \gamma = c_p/c_v$$

Putting $\rho = \tilde{\rho}(1 + \hat{\rho}/\tilde{\rho})$ etc., then $\frac{\hat{\rho}}{\tilde{\rho}} \approx \frac{1}{\gamma}\frac{\hat{p}}{\tilde{p}} - \frac{\hat{\theta}}{\tilde{\theta}}$

Hence for these buoyancy wave motions density fluctuations due to pressure changes are small compared with those due to temperature changes.

Therefore we can put

$$\hat{\rho}/\tilde{\rho} = -\hat{\theta}/\tilde{\theta}$$

and treat density as a constant except where it is coupled to gravity in the buoyancy term in the vertical momentum equation. This is known as the Boussinesq approximation.

We now define the overbar operator as an average along the x-axis, and assume that the deviations of fluid variables from their average value are small,

i.e., we write

$$u = \bar{u}_o + \varepsilon(\bar{u}_1 + u_1') + \dots$$

$$w = \varepsilon(\bar{w}_1 + w_1') + \dots$$

$$\rho = \bar{\rho}_o + \varepsilon(\bar{\rho}_1 + \rho_1') + \dots$$

$$p = \bar{p}_o + \varepsilon(\bar{p}_1 + p_1') + \dots$$

$$\theta = \bar{\theta}_o + \varepsilon(\bar{\theta}_1 + \theta_1') + \dots$$

$$\delta_x = (\bar{\delta}_x)_o + \varepsilon((\bar{\delta}_x)_1 + (\delta_x)_1') + \dots \quad \text{(etc. for } \delta_z \text{ \& } \mu)$$

Notice we have assumed that the flow is horizontal to O(1). We shall also assume that the O(1) flow is hydrostatic, i.e.,

$$\partial\bar{p}_o/\partial z = -g\bar{\rho}_o ,$$

and that the Boussinesq approximation holds.

To O(1) in the expansion, equations (i), (ii) and (iv) become, respectively

$$\frac{\partial\bar{u}_o}{\partial t} = (\bar{\delta}_x)_o \tag{0.1}$$

$$0 = (\bar{\delta}_z)_o \quad \text{(because the flow is hydrostatic)} \tag{0.2}$$

$$\frac{\partial\bar{\theta}_o}{\partial t} = \bar{\mu}_o \tag{0.3}$$

The O(ε) mean flow equations are of no interest to us here since the waves do not couple to the mean flow to O(ε). The O(ε) deviation equations are the linearized perturbation equations and take the form

$$\frac{\partial u_1'}{\partial t} + \bar{u}_o\frac{\partial u_1'}{\partial x} + w_1'\frac{\partial\bar{u}_o}{\partial z} + \frac{1}{\bar{\rho}_o}\frac{\partial p_1'}{\partial x} = -\frac{1}{2}\delta u_1' \tag{1.1}$$

$$\frac{\partial w_1'}{\partial t} + \bar{u}_o\frac{\partial w_1'}{\partial x} + \frac{1}{\bar{\rho}_o}\frac{\partial p_1'}{\partial z} - \frac{\theta_1'}{\bar{\theta}_o}g = -\frac{1}{2}\delta w_1' \tag{1.2}$$

$$\frac{\partial u_1'}{\partial x} + \frac{\partial w_1'}{\partial z} = 0 \tag{1.3}$$

$$\frac{\partial\theta_1'}{\partial t} + \bar{u}_o\frac{\partial\theta_1'}{\partial x} + w'\frac{d\bar{\theta}_o}{dz} = -\frac{1}{2}\mu\theta_1' \tag{1.4}$$

In equations (1.1) and (1.2) we have written

$$(\delta_x')_1 = -\frac{1}{2}\delta u_1' \qquad (\delta_z')_1 = -\frac{1}{2}\delta w_1'$$

which is a common form of parameterizing the effect of eddy friction. The constant δ is known as the Rayleigh friction coefficient. Similarly in (1.4), the effect of diabatic cooling $\mu\theta_1'$ has been parameterized using the Newtonian cooling coefficient μ. In (1.2) we have used the Boussinesq approximation to put $\rho_1'/\bar{\rho}_o = \theta_1'/\bar{\theta}_o$.

If we average (i), then, to $O(\varepsilon^2)$ the mean flow equation is

$$\frac{\partial\bar{u}_2}{\partial t} + \overline{w_1'\frac{\partial u_1'}{\partial z}} = (\bar{\delta}_x)_2$$

To get this we have used the Boussinesq approximation to put $\rho = \bar{\rho}_o$ in the pressure gradient term. Remember also that

$$\partial\bar{u}_o/\partial x = \partial\bar{u}_2/\partial x = 0$$

and

$$\overline{u_1'\frac{\partial u_1'}{\partial x}} = \overline{\frac{1}{2}\frac{\partial}{\partial x}(u_1')^2} = 0$$

Furthermore, using the continuity equation (1.3) we can write the $O(\varepsilon^2)$ mean flow equation as

$$\frac{\partial\bar{u}_2}{\partial t} + \frac{\partial}{\partial z}(\overline{u_1'w_1'}) = (\bar{\delta}_x)_2 \tag{2.1}$$

Hence, if the Reynolds stress $\overline{u'w'}$ varies in the vertical, then the perturbations induce an acceleration in the mean flow, to $O(\varepsilon^2)$. The right hand side of (2.1) represents the effect of mean flow viscosity.

A wave energy equation can be formed by multiplying (1.1) by u' and (1.2) by w', adding these together, and averaging, i.e.,

$$\frac{1}{2}\frac{\partial}{\partial t}(\overline{u_1'^2} + \overline{w_1'^2}) + \overline{u_1'w_1'}\frac{\partial\bar{u}_o}{\partial z} + \frac{1}{\bar{\rho}_o}\overline{u_1'\frac{\partial p_1'}{\partial x}} + \frac{1}{\bar{\rho}_o}\overline{w_1'\frac{\partial p_1'}{\partial z}} - \frac{\overline{w_1'\theta_1'}}{\bar{\theta}_o}g = -\frac{1}{2}\delta(\overline{u_1'^2} + \overline{w_1'^2})$$

Using (1.3)

$$\frac{1}{2}\frac{\partial}{\partial t}(\overline{u_1'^2} + \overline{w_1'^2}) + \overline{u_1'w_1'}\frac{\partial\bar{u}_o}{\partial z} + \frac{1}{\bar{\rho}_o}\frac{\partial}{\partial z}(\overline{w_1'p_1'}) - \frac{\overline{w_1'\theta_1'}}{\bar{\theta}_o}g = -\frac{1}{2}\delta(\overline{u_1'^2} + \overline{w_1'^2}) \tag{2.2}$$

Multiplying 1.4 x θ'

$$\frac{1}{2}\frac{\partial}{\partial t}(\overline{\theta_1'^2}) + \overline{w_1'\theta_1'}\frac{d\bar{\theta}_o}{dz} = -\frac{1}{2}\mu\overline{\theta_1'^2} \Rightarrow \frac{1}{2}\frac{\partial}{\partial t}\left(\frac{\overline{B_1'^2}}{N^2}\right) + \frac{\overline{w_1'\theta_1'}}{\bar{\theta}_o}g = -\frac{1}{2}\mu\frac{\overline{B_1'^2}}{N^2} \tag{2.3}$$

where

$$B_1' = \theta_1' g/\bar{\theta}, \quad N^2 = \frac{g}{\bar{\theta}_o}\frac{d\bar{\theta}_o}{dz}$$

Adding 2.2 and 2.3 we have

$$\frac{1}{2}\frac{\partial}{\partial t}\left(\overline{u_1'^2} + \overline{w_1'^2} + \frac{\overline{B_1'^2}}{N^2}\right) + \frac{1}{\bar{\rho}_o}\frac{\partial}{\partial z}\left(\overline{w_1' p_1'}\right) + \left(\overline{u_1' w_1'}\right)\frac{\partial u_o}{\partial z} = -\frac{1}{2}\left\{\delta\left(\overline{u_1'^2} + \overline{w_1'^2}\right) + \mu\frac{\overline{B_1'^2}}{N^2}\right\} \quad (2.4)$$

The number of variables in (1.1) to (1.4) can be reduced by introducing the y component of perturbation vorticity

$$\eta_1' = \partial w_1'/\partial x - \partial u_1'/\partial z$$

and y component of mean flow vorticity

$$\bar{\eta}_o = -\partial \bar{u}_o/\partial z$$

Then $\partial/\partial x$(1.2) $- \partial/\partial z$(1.1) gives

$$\left(\frac{\partial}{\partial t} + \bar{u}_o\frac{\partial}{\partial x}\right)\eta_1' - \left(\frac{\partial \bar{u}_o}{\partial z}\frac{\partial u_1'}{\partial x} + \frac{\partial w_1'}{\partial z}\frac{\partial \bar{u}_o}{\partial z}\right) - w_1'\frac{\partial^2 \bar{u}_o}{\partial z^2}\left(+\frac{1}{\bar{\rho}_o}\frac{\partial^2 p_1'}{\partial z \partial x} - \frac{1}{\bar{\rho}_o}\frac{\partial^2 p_1'}{\partial z \partial x}\right) - \frac{\partial B_1'}{\partial x} = -\frac{\delta}{2}\eta_1'$$

which, using the continuity equation, gives

$$\left(\frac{\partial}{\partial t} + \bar{u}_o\frac{\partial}{\partial x}\right)\eta_1' + w_1'\frac{\partial \bar{\eta}_o}{\partial z} - \frac{\partial B_1'}{\partial x} = -\frac{\delta}{2}\eta_1' \quad (1.5)$$

The thermodynamic equation, (1.4), can be written

$$\left(\frac{\partial}{\partial t} + \bar{u}_o\frac{\partial}{\partial x}\right)B_1' + N^2 w_1' = -\frac{1}{2}\mu B_1' \quad (1.6)$$

Finally, from (1.3) we can introduce a streamfunction ψ, such that

$$\left.\begin{aligned} u_1' &= -\partial\psi_1'/\partial z \\ w_1' &= \partial\psi_1'/\partial x \end{aligned}\right\} \quad \eta_1' = \nabla^2\psi_1' \quad (1.7)$$

and (1.5) and (1.6) are two coupled equations for the two perturbation variables, ψ_1' and B_1'.

To start with consider a fluid with constant (positive) static stability and constant O(1) zonal velocity $\bar{u}_o$. Suppose the fluid is bounded below by a regularly corrugated surface with sinusoidal variation in the x-direction with fixed wavelength $2\pi/k$, no variation in the y-direction, and moving in the +x-direction with fixed speed $\omega/k > 0$ (see earlier notes). Suppose also that δ and μ are equal to zero.

Using (1.7) we can substitute the expressions

$$\psi_1' = \mathrm{Re}\{\psi\, e^{i(kx - \omega t + mz)}\}$$

$$B_1' = \mathrm{Re}\{B\, e^{i(kx - \omega t + mz)}\}$$

into (1.5) and (1.6) which gives

$$-(\omega - k\bar{u}_o)(k^2 + m^2)\psi + kB = 0$$

$$(\omega - k\bar{u}_o)B = kN^2\psi$$

which can be combined to give the real dispersion relation

$$\hat{\omega} = \pm\, kN/\sqrt{k^2 + m^2} \quad (1.8)$$

so that $\hat{\omega} = \omega - k\bar{u}_o$ is the wave frequency relative to the zonal mean wind.

The vertical phase speed is

$$\omega/m = k\bar{u}_o/m \pm kN/m\sqrt{k^2 + m^2}$$

i.e., relative to the mean wind the vertical phase speed is

$$c^z = \hat{\omega}/m = \pm\, kN/m\sqrt{k^2 + m^2}$$

The vertical group velocity is

$$c_g^z = \partial\hat{\omega}/\partial m = \partial\omega/\partial m = \mp\, mkN/(k^2 + m^2)^{3/2} = -c^z\frac{m^2}{k^2 + m^2} \quad (1.9)$$

Notice that downward phase propagation in a frame moving with the fluid $\Rightarrow$upward group velocity, (and vice versa)

Other properties of note are

(1) From the dispersion relation wavelike solutions only obtain if $N^2 \geq \hat{\omega}^2 > 0$.

(2) When $\hat{\omega} \to 0$, then, according to the dispersion relation, $m \to \infty$ (i.e., the vertical wavelength $\to 0$). When $\hat{\omega} \to N$ then $m \to 0$, i.e., phase lines become vertically oriented. In general if $\hat{\omega}^2$ decreases, then m^2 must increase, and the lines of constant phase become more horizontally aligned.

(3) A straightforward calculation gives $\partial(c^z)^2/\partial m^2 < 0$ if $\hat{\omega}^2 < 2/3\ N^2$. In other words providing $\hat{\omega}^2 < 2/3\ N^2$ then if m^2 increases, $(c^z)^2$ decreases. Combining this with the result in (2), then $(c_g^z)^2$ varies directly with $\hat{\omega}^2$ if $\hat{\omega}^2 < 2/3\ N^2$.

Now suppose that instead of the basic state mean flow having no vertical shear and the waves are inviscid, we allow, in the spirit of the WKBJ approximation, a small amount of vertical shear $\partial\bar{u}_o/\partial z$ (i.e., a slowly varying mean wind $\bar{u}_o$) and a small amount of Rayleigh friction and Newtonian cooling. Formally, this can be achieved by introducing a small parameter $\tau << 1$ and introducing a long space variable

$$Z = \tau z$$

so that

$$\bar{u} = \bar{u}(Z) \qquad \delta = \tau\delta_o \qquad \mu = \tau\mu_o \qquad (\delta_o, \mu_o = O(1))$$

and seek WKBJ solutions

$$\psi_1' = \mathrm{Re}\left\{\psi(Z)e^{i(kx - \omega t + \phi/\tau)}\right\} \qquad B_1' = \mathrm{Re}\left\{B(Z)e^{i(kx - \omega t + \phi/\tau)}\right\}$$

where

$$m(Z) = \partial\phi/\partial Z \left(= \frac{1}{\tau}\frac{\partial\phi}{\partial z}\right)$$

Now if we substitute these solutions into 1.5, 1.6 and 1.7, then, to lowest order in τ

$$\frac{\partial}{\partial z}\left\{\psi(Z)e^{i(kx - \omega t + \phi/\tau)}\right\} = i\frac{1}{\tau}\frac{\partial\phi}{\partial z}\psi(Z)e^{i(kx - \omega t + \phi/\tau)} + \tau\frac{\partial\psi}{\partial Z}e^{i(kx - \omega t + \phi/\tau)}$$

$$= i\,m(Z)\,\psi(Z)e^{i(kx - \omega t + \phi/\tau)} + O(\tau)$$

i.e., to lowest order in τ there is no difference between the WKBJ solution and the elementary solution with m = constant. In particular, the dispersion relation 1.9 and conclusions (1)-(3) will all hold to lowest order in τ.

A difference arises; however, when we consider the energy equation, which, since we assume a steady state (i.e., no time variation in wave amplitudes) becomes

$$\frac{1}{\bar{\rho}_o}\frac{\partial}{\partial z}\left(\overline{w_1'p_1'}\right) + \left(\overline{u_1'w_1'}\right)\frac{\partial\bar{u}_o}{\partial z} = -\frac{1}{2}\left\{\delta\left(\overline{u_1'^2} + \overline{w_1'^2}\right) + \mu\frac{\overline{B_1'^2}}{N^2}\right\} \qquad (2.5)$$

Now since

$$u_1' = -\partial\psi_1'/\partial z$$

$$w_1' = \partial\psi_1'/\partial x$$

then

$$\left(\overline{u_1'^2}\right) + \left(\overline{w_1'^2}\right) = \overline{\left(\frac{\partial\psi_1'}{\partial x}\right)^2} + \overline{\left(\frac{\partial\psi_1'}{\partial z}\right)^2} = (k^2 + m^2)|\psi|^2/2 \qquad (2.6)$$

Since $\mu = O(\tau)\mu_o$, then, from 1.6, to lowest order in τ

$$(\omega - k\bar{u}_o)B - kN^2\psi = 0$$

i.e.,

$$\frac{\overline{B_1'^2}}{N^2} = \frac{|B|^2}{2N^2} = \frac{|\psi|^2k^2N^2}{2\hat{\omega}^2} = (k^2 + m^2)|\psi|^2/2 \qquad (2.7)$$

using the dispersion relation (1.8).

Again since $\delta = O(\tau)\delta_o$, then to lowest order in τ 1.1 is

$$\left(\frac{\partial}{\partial t} + \bar{u}_o\frac{\partial}{\partial x}\right)u_1' = -\frac{1}{\bar{\rho}_o}\frac{\partial p_1'}{\partial x}$$

i.e.,

$$\hat{\omega}u_1' = -\frac{k}{\bar{\rho}_o}p_1'$$

or

$$P = -\frac{\bar{\rho}_o\hat{\omega}}{k}(-im\psi) \qquad \text{where } p_1' = \mathrm{Re}[P(z)e^{i(kx - wt + \phi/\tau)}]$$

so that

$$\overline{w_1'p_1'} = -\bar{\rho}_o m\hat{\omega}|\psi|^2/2 \qquad (2.8)$$

Finally

$$\overline{u_1'w_1'} = -mk|\psi|^2/2 \qquad (2.9)$$

Substituting 2,6, 2.7, 2.8 and 2.9 into 2.5 and defining

$$\alpha = \frac{1}{2}(\delta + \mu)$$

we get

$$\frac{\partial}{\partial z}(m\hat{\omega}|\psi|^2) + mk|\psi|^2\frac{\partial\bar{u}_o}{\partial z} = \alpha(k^2 + m^2)|\psi|^2 \qquad (2.10)$$

Now for the simple case with no shear and no dissipation then both sides of this equation are trivially zero since m and $|\psi^2|$ would be constants. With weak shear and weak dissipation this equation gives an expression for how wave amplitudes must vary with height. Notice that 2.10 can be written purely in terms of the long space coordinate (since m, ω, u_o and ψ are all functions of Z only) i.e.,

$$\frac{d}{dZ}(m\hat{\omega}|\psi|^2) + mk|\psi|^2\frac{d\bar{u}_o}{dZ} = \alpha_o(k^2 + m^2)|\psi|^2 \qquad (2.11)$$

where $\alpha = \tau\alpha_o$.

Now if we define a quantity

$$A = (k^2 + m^2)|\psi|^2/\hat{\omega}$$

called wave-action, then from the definition of group velocity c_g^z we can write (from (1.8) and (1.9))

$$c_g^z A = - m|\psi|^2$$

and 2.11 can be written as

$$\frac{d}{dZ}(c_g^z A\hat{\omega}) + kc_g^z A \frac{d\bar{U}_o}{dZ} = - \alpha_o A \hat{\omega}$$

But

$$\frac{d\hat{\omega}}{dZ} = \frac{d\omega}{dZ} - k\frac{d\bar{U}_o}{dZ} = - k\frac{d\bar{U}_o}{dZ}$$

Hence

$$\frac{d}{dZ}(c_g^z A) = - \alpha_o A \qquad (2.12)$$

which is a differential equation for the depletion of wave-action due to the combined effects of dissipation and diabatic cooling.

Writing 2.12 as

$$\frac{d}{dZ}(c_g^z A) = - (c_g^z A)/D$$

where $D = c_g/\alpha_o$, then the solution

$$Ac_g^z\Big|_z = Ac_g^z\Big|_{z=0} e^{-\int_o^z D^{-1}dz}$$

of 2.12 is easily obtained. Furthermore, since the wave momentum flux

$$\overline{u_1'w_1'} = - \frac{1}{2} km|\psi|^2 = \frac{1}{2} kAc_g^z$$

then 2.6 can also be written as

$$\overline{u_1'w_1'}\Big|_z = \overline{u_1'w_1'}\Big|_{z=0} e^{-\int_o^z D^{-1}dz}$$

and according to 2.1, the waves induce an $O(\epsilon^2)$ acceleration

$$-\frac{\partial}{\partial z}(\overline{u_1'w_1'}) = D^{-1}\,\overline{u_1'w_1'}\Big|_{z=0} e^{-\int_o^z D^{-1}dz}$$

to the mean flow.

The quantity D is a height scale for wave dissipation. If α is small or c_g is large (so that D is large) the waves propagate a large depth before the momentum flux is substantially depleted. Consequently the mean flow is accelerated weakly over a large depth of the fluid. Conversely if α is large or c_g is small then the waves are dissipated over a shallow depth of the fluid and the mean flow acceleration is concentrated in that shallow depth.

We now recall the following pieces of information:

(1) For fixed α, the dissipation height scale D varies directly with c_g.

(2) For $\hat{\omega}^2 < 2/3\ N^2$, c_g^z varies directly with $\hat{\omega}$.

(3) For waves with positive (Doppler shifted) frequency $\hat{\omega}$, wave, mean-flow interaction through wave-dissipation will decrease $\hat{\omega}$ (i.e., the wave momentum flux will tend to accelerate the mean flow to the speed of the corrugated boundary which forces the waves).

This gives us a positive feedback loop. If $\hat{\omega}$ decreases then from (2) c_g^z decreases, so from (1) D decreases. The waves therefore dissipate over a smaller depth above the lower boundary. Hence the mean flow accelerates more strongly in this region -- hence $\hat{\omega}$ decreases more strongly in this region: so c_g^z decreases more strongly -- hence D decreases still further.....until finally $\hat{\omega}$ is reduced to zero immediately above the lower boundary and no further wave propagation can occur.

A surface where $\hat{\omega} = 0$ is called a critical surface, and according to the wave dispersion relation, $m^2 \to \infty \Rightarrow c_g^z \to 0$, i.e., $D \to 0$. Hence for any non-zero value of α, critical layers are (for linear theory) strong absorbers of wave-activity.

If the boundary executes a standing wave oscillation

$$z = A \sin k(x + ct) + A \sin k(x - ct)$$

where $c = \omega/k$, then even when the component moving with phase speed $+c$ is trapped, the component moving with phase speed $-c$ is not trapped -- relative to this phase speed the Doppler shifted frequency is 2ω. This wave can induce wave mean flow deceleration, resulting in the vacillating mean flow described in the earlier notes, and demonstrated by the Plumb and McEwan experiment.

WKBJ analysis is, in fact, rather more powerful than we have so far been able to show. It turns out that it is possible to carry out a WKBJ analysis to the full nonlinear internal gravity wave equations. Under such circumstances wave, mean-flow interaction would be accounted for to all orders of τ, and due to such interaction the waves and mean-flow would be slowly varying in time. Under these circumstances 2.12 generalizes to

$$\frac{\partial A}{\partial T} + \frac{\partial}{\partial Z}(c_g^z A) = -\alpha_o A \qquad (2.13)$$

where $A = A(T,Z)$

and $T = \mu t$

Equation 2.13 is the full equation for conservation of wave action. In the absence of any dissipation or diabatic cooling then

$$\frac{\partial A}{\partial T} + \frac{\partial}{\partial Z}(c_g^z A) = 0$$

so that the rate of change of wave-action in any depth $\Delta z = z_2 - z_1$ of the fluid

$$= \frac{\partial}{\partial t}\int_{z_1}^{z_2} A\,dz = \tau\int_{z_1}^{z_2}\frac{\partial A}{\partial T}\,dz = -\tau\int_{z_1}^{z_2}\frac{\partial}{\partial Z}(c_g^z A)dz$$

$$= -\int_{z_1}^{z_2}\frac{\partial}{\partial z}(c_g^z A)dz = c_g^z A\Big|_{z=z_1} - c_g^z A\Big|_{z=z_2}$$

i.e., the wave-action in any depth Δz will change solely due to the advection of wave-action through the boundary of Δz by the group velocity c_g^z.

Appendix

1. Non acceleration theorem for internal gravity waves.

Multiply (1.6) by B_1' and average

$$\frac{1}{2}\frac{\partial}{\partial t}\overline{B_1'^2} + \overline{w_1'B_1'}N^2 = -\frac{1}{2}\mu\,\overline{B_1'^2} \qquad (A.1)$$

Multiply (1.6) by η_1' and average

$$\overline{\eta_1'\frac{\partial B_1'}{\partial t}} + \bar{u}_o\,\overline{\eta_1'\frac{\partial B_1'}{\partial x}} + N^2\,\overline{w_1'\eta_1'} = -\frac{1}{2}\mu\,\overline{B_1'\eta_1'} \qquad (A.2)$$

Multiply (1.5) by B_1' and average

$$\overline{B_1'\frac{\partial \eta_1'}{\partial t}} + \bar{u}_o\,\overline{B_1'\frac{\partial \eta_1'}{\partial x}} + \overline{w_1'B_1'}\frac{\partial \bar{\eta}_o}{\partial z} = -\frac{1}{2}\delta\,\overline{B_1'\eta_1'} \qquad (A.3)$$

Add A2 and A3

$$\frac{\partial}{\partial t}(\overline{\eta_1'B_1'}) + \overline{w_1'B_1'}\frac{\partial \bar{\eta}_o}{\partial z} + \overline{w_1'\eta_1'}N^2 = -\alpha\,\overline{B_1'\eta_1'} \qquad (A.4)$$

From (A.1), $\overline{w_1'B_1'}$ is zero if the waves are steady and non-dissipative. Hence, from (A.4) $\overline{w_1'\eta_1'}$ is zero if the waves are steady and non-dissipative.

But

$$\overline{w_1'\eta_1'} = -\overline{w_1'\partial u_1'}/\partial z = -\frac{\partial}{\partial z}(\overline{u_1'w_1'})$$

Hence $(\partial/\partial z)(\overline{u_1'w_1'})$ is non-zero if the waves are steady and non-dissipative. From (2.1)

$$\frac{\partial \bar{u}_2}{\partial t} + \frac{\partial}{\partial z}(\overline{u_1'w_1'}) = (\bar{\delta}_x)_2$$

Hence to $O(\epsilon^2)$ the waves cannot change the mean zonal flow if they are steady and non-dissipative.

This is called the non-acceleration theorem for internal gravity waves. There is a similar theorem for quasigeostrophic waves.

2. Conservation of wave-action for a basic state which is slowly varying in time.

Put $T = \tau t$

$Z = \tau z \qquad \tau << 1$

$\bar{u}_o = \bar{u}_o(Z,T) \qquad \alpha = \tau\alpha_o$

and seek WKBJ solutions

$$\psi_1' = \mathrm{Re}\ \{\psi(Z,T)e^{i(kx+\phi(Z,T)/\tau)}\}$$

$$B_1' = \mathrm{Re}\ \{B(Z,T)e^{i(kx+\phi(Z,T)/\tau)}\}$$

and

$$\omega(Z,T) = -\partial\phi/\partial T \qquad m(Z,T) = \partial\phi/\partial Z$$

n.b.

$$\partial\omega/\partial Z + \partial m/\partial T = 0\ .$$

With $\hat{\omega} = \omega - k\bar{u}_o$, then since, from the dispersion relation $\hat{\omega} = \hat{\omega}(m)$

$$\frac{\partial\hat{\omega}}{\partial T} = \frac{\partial\hat{\omega}}{\partial m}\frac{\partial m}{\partial T} = c_g^z\frac{\partial m}{\partial T} = -c_g^z\frac{\partial\omega}{\partial Z} \qquad (A.5)$$

from the above relation.

The energy equation (2.4) is

$$\frac{\partial}{\partial t}\{(k^2+m^2)|\psi|^2\} - \frac{\partial}{\partial z}\{m\hat{\omega}|\psi|^2\} - mk|\psi|^2\frac{\partial\bar{u}_o}{\partial Z} = -\alpha\ (k^2+m^2)|\psi|^2 \qquad (A.6)$$

As before define the wave-action

$$A = (k^2+m^2)|\psi|^2/\hat{\omega} \Rightarrow c_g^z A = -m|\psi|^2$$

Substituting this into (2.6) and noting that each term is $O(\tau)$ then

$$\frac{\partial}{\partial T}\{A\hat{\omega}\} + \frac{\partial}{\partial Z}\{c_g^z A\hat{\omega}\} + c_g^z Ak\frac{\partial\bar{u}_o}{\partial Z} = -\alpha_o A\hat{\omega} \qquad (A.7)$$

But using (A.5) and the identity

$$k\frac{\partial\bar{u}_o}{\partial Z} = \frac{\partial\omega}{\partial Z} - \frac{\partial\hat{\omega}}{\partial Z} \Rightarrow c_g^z k\frac{\partial\bar{u}_o}{\partial Z} = -\frac{\partial\hat{\omega}}{\partial T} - c_g^z\frac{\partial\hat{\omega}}{\partial Z}$$

(A.7) becomes, dividing by

$$\frac{1}{\hat{\omega}}\frac{\partial}{\partial T}(A\hat{\omega}) - A\frac{1}{\hat{\omega}}\frac{\partial\hat{\omega}}{\partial T} + \frac{1}{\hat{\omega}}\frac{\partial}{\partial Z}\{c_g^z A\hat{\omega}\} - c_g^z A\frac{1}{\hat{\omega}}\frac{\partial\hat{\omega}}{\partial Z} = -\alpha_o A$$

which can be rearranged to give

$$\boxed{\frac{\partial A}{\partial T} + \frac{\partial}{\partial Z}(c_g^z A) = -\alpha_o A}$$

which is an equation for conservation of wave-action in the absence of dissipation.

Fundamental to dynamical meteorology is the equation for conservation of potential vorticity, Q. In its most general form Ertel's theorem (see eg Pedlosky) states that

1. If Λ is a conserved scalar (ie $d\Lambda/dt=0$)
2. $\Lambda=\Lambda(\rho,p)$ or fluid is barotropic (ie $\nabla\rho\times\nabla p=0$)
3. No friction

then

$$Q=\rho^{-1}\,\omega_a.\nabla\Lambda$$

is conserved, ie $dQ/dt=0$. Q is called potential vorticity, with $\omega_a=\nabla\times u_a$ the absolute vorticity. Here the subscript "a" denotes an absolute (inertial) frame of reference. If $\omega=\nabla\times u$ is vorticity in a frame rotating with angular velocity Ω, $\omega_a=\omega+2\Omega$.

Sketch proof

There is a very close relationship between Ertel's theorem, and Kelvin's circulation theorem, as outlined below.

Suppose A is a material surface (ie a surface which follows a fixed set of fluid elements)

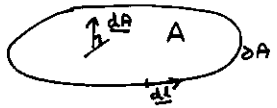

Kelvin's circulation theorem (see eg Holton,) states that

$$\frac{d\Gamma_a}{dt}=-\int_{\partial A}\rho^{-1}\nabla p\times dl=\int_A\frac{\nabla\rho\times\nabla p}{\rho^2}.dA$$

where Γ_a is the (absolute) circulation

$$\Gamma_a\equiv\int_{\partial A}u_a\times dl=\int_A\omega_a.dA\qquad\text{(by Stokes' theorem)}$$

Now since $d\Lambda/dt=0$ then $\Lambda=\Lambda_0$ is a material surface. Let $A\subset\Lambda_0$ so that dA is parallel to $\nabla\Lambda$.

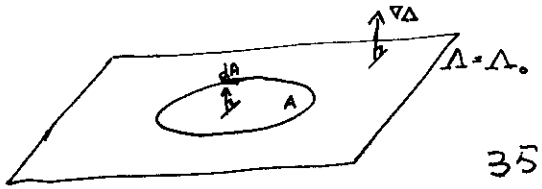

Since, also,

$$\Lambda=\Lambda(\rho,p)$$
$$\nabla\Lambda=\frac{\partial\Lambda}{\partial\rho}\nabla\rho+\frac{\partial\Lambda}{\partial p}\nabla p$$
ie $(\nabla\rho\times\nabla p).\nabla\Lambda=0\quad\therefore\quad(\nabla\rho\times\nabla p).dA=0$
$$\Rightarrow\frac{d\Gamma_a}{dt}=0$$

ie the absolute circulation is conserved on $\Lambda=\Lambda_0$

Now consider a small area δA (moving with the fluid) on $\Lambda=\Lambda_0$

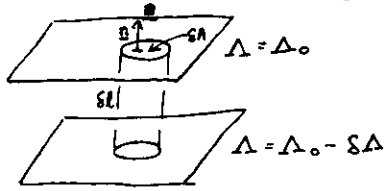

n is the unit normal

and a small cylinder with mass $\delta m=\rho\,\delta A\,\delta l$ with ends lying on two Λ surfaces.

Since $|\nabla\Lambda|=\delta\Lambda/\delta l$

then $\delta m=\rho\,\delta A\,\delta\Lambda/|\nabla\Lambda|$

ie $\delta A=\frac{1}{\rho}|\nabla\Lambda|\,\delta m/\delta\Lambda$

Kelvin's circulation theorem for the small area states that

$$\frac{d}{dt}(\omega_a.n\,\delta A)=0\qquad\xi\quad(dA=n\,\delta A)$$

ie $$\frac{d}{dt}\left(\frac{\omega_a.\nabla\Lambda}{\rho}\,\frac{\delta m}{\delta\Lambda}\right)=0\qquad(\nabla\Lambda=n|\nabla\Lambda|)$$

But δm and $\delta\Lambda$ are constants of the motion, by construction, hence required result ie

$$\frac{d}{dt}\left(\frac{\omega_a.\nabla\Lambda}{\rho}\right)=0$$

For dynamical meteorology, most important application is when Λ = potential temperature, θ. For adiabatic flow $d\theta/dt=0$ where $\theta=T\left(\frac{1000}{p}\right)^{\kappa}$ where κ is the ratio of specific heats.

Can see qualitatively how Rossby waves are forced by topography. For large scale atmospheric motions

$$\rho^{-1}\,\underline{\omega}_a \cdot \nabla\theta \simeq \rho_*^{-1}\left(\zeta + f\right)\frac{d\theta}{dz}$$

(ζ = vertical component of $\underline{\omega}$, f = vertical component of $2\underline{\Omega}$ - for further comments about scaling, see below)

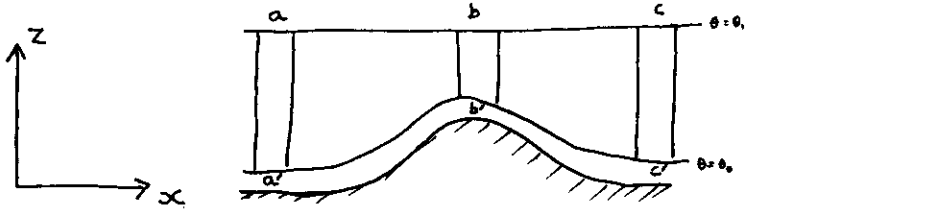

$\zeta > 0 \Rightarrow$ cyclonic vorticity

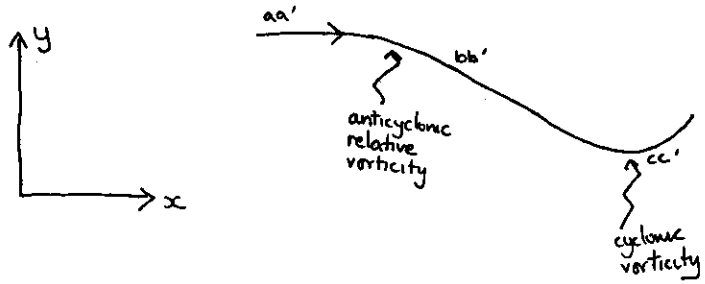

Suppose $\zeta_{aa'} = 0$

Since $\left(\frac{d\theta}{dz}\right)_{bb'} > \left(\frac{d\theta}{dz}\right)_{aa'}$, $\quad (f+\zeta)_{bb'} < f_{aa'}$

ie the column of air acquires anticyclonic relative vorticity as it moves over the mountain, and moves south

Since $\left(\frac{d\theta}{dz}\right)_{cc'} = \left(\frac{d\theta}{dz}\right)_{aa'}$

then $f_{cc'} + \zeta_{cc'} = f_{aa'}$

But $f_{cc'} < f_{aa'}$ so $\zeta_{cc'} > 0$ ie the column of air acquires cyclonic vorticity and moves back to its original latitude.

Hence the gradient of f with latitude acts as a restoring force for air parcels. The concept of the Rossby waves is based on this idea.

An analytic model of this effect can be made using the quasi-geostrophic scaling to the Ertel potential vorticity equations. We choose the following scales:

1. A horizontal length scale $L = 10^6$ m.
2. A horizontal velocity $U = 10\ \mathrm{ms}^{-1}$.
3. A vertical depth $\mathcal{D} = 10^4$ m.
4. A time scale U/L (equal to the advective time).

Also $f = 10^{-4}\ \mathrm{s}^{-1}$

$g = 10\ \mathrm{ms}^{-2}$

$a = 10^7$ m (radius of earth)

$c^2 = \gamma RT \sim 10^5\ \mathrm{m}^2\,\mathrm{s}^{-1}$ (speed of sound squared)

So $R_o = U/fL = 10^{-1}$ Rossby number (ratio of inertial to Coriolis acceleration)

$\delta = \mathcal{D}/L = 10^{-2}$ aspect ratio

$\tilde{\delta} = L/a = 10^{-1}$

$Ma^2 = (U/c)^2 = 10^{-3}$

Suggest scaling according to

1. motions slow compared with speed of sound $Ma \ll 1$
2. thin atmosphere $\delta \ll 1$
3. slow motions compared with planetary time scale and small scale compared with planetary radius. $R_o \ll 1$, $\tilde{\delta} \ll 1$

To lowest order in this scaling, the vertical momentum equation gives the hydrostatic approximation and the horizontal momentum equation gives the geostrophic approximation,

$$v = \frac{\partial \psi}{\partial x}\Big|_p \qquad u = -\frac{\partial \psi}{\partial y}\Big|_p \qquad \phi = \text{geopotential}$$

where $|_p$ means 'evaluated on an isobaric level' and ψ is the geostrophic stream function $\psi = \phi/f_0$. (f_0 is some constant mid-latitude value). From this and the continuity equation we can get an estimate of vertical velocity W , ie

$$w = R_0 \, U \, D/L$$

The factor R_0 in this expression signifies that the geostrophic wind is quasi-non-divergent.

In order to balance the thermodynamic equation it is necessary that the static stability $d\theta_0/dz$, satisfies $\left(z = -H \ln (p/1000) \right)$

$$\frac{d\theta_0}{dz} = R_0 \frac{\theta_0}{D} \qquad \text{(OK from observations in midlatitudes)}$$

or

$$B = N^2 D^2 / f^2 L^2 = O(1) \qquad \left(N^2 = \frac{RT_0}{H} \frac{d\ln\theta}{dz} \right)$$

where

$$\theta = \theta_0(z) + \theta'(x,y,z,t) \qquad \text{(similarly for } \rho_0\text{)}$$

and θ_0 is the potential temperature pertaining to an exactly hydrostatic atmosphere (ie one with no motion). $\left(\rho_0 = \exp(-z/H) \right)$

With this scaling the equation for conservation of Ertel's potential vorticity becomes, to lowest order (see Pedlosky)

$$\frac{d_h q}{dt} = 0$$

where

$$q = f_0 + \beta y + \zeta_g + \frac{f_0}{\rho_0} \frac{\partial}{\partial z} \left(\rho_0 \frac{\theta'}{d\theta/dz} \right)$$

is the quasi-geostrophic potential vorticity. In this expression ζ_g is the relative vorticity expressed using the geostrophic wind, $f_0 + \beta y$ is the Taylor expansion for f in terms of the small parameter $\tilde{\delta} = L/a$, and $d_h/dt = \partial/\partial t + \underline{u}_g \cdot \nabla$

Using the geostrophic stream function

$$\frac{\partial \phi}{\partial \rho} = -\frac{1}{\rho} \Rightarrow T = -\frac{H}{R} f_0 \frac{\partial \psi}{\partial z}$$

and the hydrostatic approximation we can write the equation for conservation of potential vorticity as

$$\frac{\partial q}{\partial t} + J(\psi, q) = 0$$

where

$$J(a,b) = \frac{\partial a}{\partial x}\frac{\partial b}{\partial y} - \frac{\partial a}{\partial y}\frac{\partial b}{\partial x}$$

and

$$q = f_0 + \beta y + \nabla^2 \psi + \frac{f_0^2}{\rho_0} \frac{\partial}{\partial z} \left\{ \frac{\rho_0}{N^2} \frac{\partial \psi}{\partial z} \right\}$$

and $\rho_0 = \exp(-z/H)$

$H \sim 7$ km is a typical scale-height.

<u>Example of the use of the quasi-geostrophic potential vorticity equation - excitation of orographically forced Rossby waves.</u>

Consider simplest case viz linearise about uniform flow.

Write each variable as a sum of a zonal mean + a deviation

$$q = \bar{q} + q'$$
$$u = \bar{u} + u'$$
$$v = \bar{v} + v'$$

etc.

Here $\bar{v} = 0$, $\bar{u} = u_0$,

so

$$\frac{\partial q'}{\partial t} + u_0 \frac{\partial q'}{\partial x} + v'\beta = 0$$

Boundary condition for steady orographic forcing. Let h_T = height of orography with $h_T = h_0 \exp(ikx)$

$$w = dh_T/dt \quad \text{at} \quad z = 0$$

$= \left(\frac{\partial}{\partial t} + \underline{v}\cdot\nabla\right) h_T$

$= u_0 \partial h_T / \partial x$ in linearised form (ie small h_T)

$= ik u_0 h_T$

at z=o in linearised form.

Look for stationary wave solutions of the form (assume no y variation for simplicity)

$$\psi' \sim \tilde{\psi}(z) \exp(ikx) \qquad 1)$$

in the linearised potential vorticity equation, giving

$$\frac{f_0^2}{\rho_0}\frac{\partial}{\partial z}\left(\frac{\rho_0}{N^2}\frac{\partial \tilde{\psi}}{\partial z}\right) = \tilde{\psi}\left(k^2 - \beta/\bar{u}_0\right)$$

since $v' = \partial\psi'/\partial x$

$q' = \nabla^2\psi' + \frac{f_0}{\rho_0}\frac{\partial}{\partial z}\left(\frac{\rho_0}{N^2}\frac{\partial \psi}{\partial z}\right)$

$\partial/\partial t = 0$

Putting

$$\xi = \psi' \exp(-z/2H) \qquad 2)$$

gives

$$\frac{\partial^2 \xi}{\partial z^2} = \frac{N^2}{f_0^2}\left(k^2 + \gamma^2 - \beta/\bar{u}_0\right)$$

where

$$\gamma = f_0/2NH$$

If

$$k^2 + \gamma^2 - \beta/\bar{u} < 0$$

ie $$0 < \bar{u} < \beta/k^2+\gamma^2$$

then vertically propagating solutions will exist ie

$$\xi = \xi_0 \exp(imz) \qquad 3)$$

with

$$m = \pm \frac{N}{f_0}\left(\beta/u_0 - k^2 - \gamma^2\right)^{1/2} \qquad 4)$$

cf summer stratosphere $\bar{u} < 0$, no wave propagation from troposphere: winter stratosphere, upward propagation for only low wavenumbers.

We can express ξ_0 in terms of h_T using the thermodynamic equation together with the boundary condition. From the thermodynamic equation (using the fact that from the hydrostatic relationship $T' = -\frac{H}{R} f_0 \partial\psi'/\partial z$)

$$u_0 \frac{\partial}{\partial x}\left(\frac{\partial \psi'}{\partial z}\right) + \frac{N^2}{f_0} w' = 0$$

At $z = 0$ from boundary condition

$$\frac{\partial}{\partial x}\left(\frac{\partial \psi'}{\partial z}\right) + \frac{N^2}{f_0}\frac{\partial h_T}{\partial x} = 0$$

substituting for ψ' in terms of ξ_0 (using 1), 2) and 3) we get

$$\left(im + \frac{1}{2H}\right)\xi_0 = -\frac{N^2 h_T}{f_0}$$

Hence, the final solution is for a propagating solution

$$\psi' = -\exp(z/2H)\frac{N^2 h_T}{f_0}\left(im + \frac{1}{2H}\right)^{-1}\exp(imz + ikx)$$

where

$$m = \frac{N}{f_0}\left(\frac{\beta}{\bar{u}_0} - k^2 - \frac{f_0^2}{4N^2H^2}\right)^{1/2}$$

Generalisation for Rossby wave propagation in y and z plane with general basic state and spherical geometry with wave solns of the form

$$\psi' \sim \exp(ikx + ily + imz)$$

can show (see Palmer, 1982) that the generalisation of the dispersion relation 4) is

$$l^2 + \frac{f^2}{N^2}m^2 = Q^2$$

where

$$Q^2 = \frac{\partial \bar{q}/\partial y}{\bar{u}} - \frac{k^2}{r^2\cos^2\phi} - \frac{f^2}{4H^2N^2}$$

$\frac{\partial \bar{q}}{\partial y} = \frac{f}{r}$

$-\left\{\frac{1}{\cos\phi}(\bar{v}\cos\phi)_y\right\}_y$

$+f\left(\frac{\bar{\theta}_y}{\bar{\theta}_z}e^{-z/H}\right)_z e^{z/H}$

is the refractive index squared. Alternatively, defining a vector

$$\underset{\sim}{F} = \tfrac{1}{2}k\exp(z/H)|\Phi|^2\left(\frac{l}{f^2}, \frac{m}{N^2}\right)$$

in the (y,z) plane the dispersion relation can be written as

$$|\underline{F}|^2 \propto Q^2 \qquad 5)$$

Wave propagation only occurs if $Q^2 > 0$. More generally we can show that

1. $\underline{F}$ is parallel to the group velocity.
2. From 5), trajectories of $\underline{F}$ curve up the gradient of $Q/\sin^2\phi$
3. $\underline{F}$ can be written in the form

$$\underline{F} = r\cos\phi\, e^{-z/H}\left(-\overline{u'v'},\ f\,\overline{v'\theta'}/\bar{\theta}_z\right)$$

and is known as the Eliassen-Palm flux. In the stratosphere $\underline{F}$ can be constructed from observations of satellite radiances + 100 mb geopotential height data.

The Elassen-Palm flux is also an important diagnostic for wave, mean-flow interaction since $\nabla.\underline{F}$ is a measure of the eddy feedback on the mean flow. In the transformed Eulerian mean equations

$$\frac{\partial \bar{u}}{\partial t} = f\bar{v}^* + \frac{e^{z/H}}{r\cos\phi}\nabla.F$$

$$\frac{\partial \bar{\theta}}{\partial t} = -\bar{\theta}_z \bar{w}^* + \bar{Q}$$

$(\bar{v}^*, \bar{w}^*)$ is the residual meridional circulation (see Edmon et al, JAS, 37, 2600-2616, 1980) defined by

$$\bar{v}^* = \bar{v} - e^{z/H}\frac{\partial}{\partial z}\left(e^{-z/H}\,\overline{v'\theta'}/\bar{\theta}_z\right)$$

$$\bar{w}^* = \bar{w} + \frac{1}{r\cos\phi}\frac{\partial}{\partial\phi}\left(\cos\phi\ \overline{v'\theta'}/\bar{\theta}_z\right)$$

As explained above, for steady conservative linear waves $\bar{v}^* = \bar{w}^* = 0$ (unlike $\bar{v}, \bar{w}$), hence and they approximate to Lagrangian mean velocities.

Also, for steady conservative waves, $\nabla.\underline{F} = 0$. This is the non-acceleration theorem ie there is no eddy-induced acceleration of the mean flow when the waves are steady and conservative.

43

Conclusions

The most straightforward interpretation of the power spectrum of total irradiance data is that the low-l p-modes behave like independent, randomly excited harmonic oscillators. The damping time $\tau \simeq 2$ days of the multiplet substates, inferred directly from the line widths of the main $l = 0$ modes and indirectly from the scatter in the power of the modes, is incompatible with the previous observation of rotationally split components. The composite width of the unresolved $l = 1$ peaks in our spectrum is consistent with either the amount of splitting (0.75 μHz per m-state) claimed by Claverie *et al.*, which we take as an upper bound, or with the splitting expected from uniform rotation at a rate of ~0.43 μHz. We conclude that the precise rotation rate of the solar interior is still an open question.

We thank W. A. Coles and P. Delache for useful discussions and R. C. Willson for providing both reduced ACRIM data and continuing assistance. This work was supported by NASA under grant NSG 7161.

Received 30 June; accepted 10 August 1983.

1. Claverie, A., Isaak, G. R., McLeod, C. P., van der Raay, H. B. & Roca Cortes, T. *Nature* **282**, 591–594 (1979).
2. Ulrich, R. K. & Rhodes, E. J. Jr *Astrophys. J.* **265**, 551–563 (1983).
3. Claverie, A., Isaak, G. R., McLeod, C. P., van der Raay, H. B. & Roca Cortes, T. *Nature* **293**, 443–445 (1981).
4. Ledoux, P. *Astrophys. J.* **114**, 373–384 (1951).
5. Isaak, G. R. *Nature* **296**, 130–131 (1982).
6. Dicke, R. H. *Nature* **300**, 693–697 (1982).
7. Gough, D. O. *Nature* **298**, 350–354 (1982).
8. Gree, G., Fossat, E. & Pomerantz, M. *Solar Phys.* **82**, 55–66 (1983).
9. Willson, R. C. *Appl. Opt.* **18**, 179–188 (1979).
10. Willson, R. C. & Hudson, H. S. *Astrophys. J. Lett* **244**, L185–189 (1981).
11. Woodard, M. & Hudson, H. *Solar Phys.* **82**, 67–73 (1983).
12. Woodard, M., Hudson, H. & Willson, R. in *Pulsations in Classical and Cataclysmic Variable Stars* (eds Cox, J. P. & Hansen, C. J.) 152–156 (JILA, Boulder, 1982).
13. Gough, D. O. in *Nonradial and Nonlinear Stellar Pulsation* (eds Hill, H. A. & Dziembowski, W. A.) 273 (Springer, Berlin, 1980).
14. Christensen-Dalsgaard, J. & Frandsen, S. *Solar Phys.* **82**, 469–486 (1983).
15. Goldreich, P. & Keeley, D. A. *Astrophys. J.* **212**, 243–251 (1977).
16. Duvall, T. L. Jr & Harvey, J. W. *Nature* **302**, 24–27 (1983).
17. Shibahashi, H. & Osaki, Y. *Publ. astr. Soc. Japan* **33**, 713–719 (1981).
18. Gabriel, M., Scuflaire, R. & Noels, A. *Astr. Astrophys.* **110**, 50–53 (1982).
19. Gough, D. O. in *Pulsations in Classical and Cataclysmic Variable Stars* (eds Cox, J. P. & Hansen, C. J.) 117–137 (JILA, Boulder, 1982).
20. Christensen-Dalsgaard, J. & Frandsen, S. *Solar Phys.* **82**, 165–204 (1983).
21. Delache, P. & Scherrer, P. *Nature* (in the press).

Breaking planetary waves in the stratosphere

M. E. McIntyre* & T. N. Palmer†

* Department of Applied Mathematics and Theoretical Physics, University of Cambridge, Cambridge CB3 9EW, UK
† Meteorological Office, Bracknell, Berks RG12 2SZ, UK

Satellite-borne IR radiometers are turning the Earth's stratosphere into one of the best available outdoor laboratories for observing the large-scale dynamics of a rotating, heterogeneous fluid under gravity. New insight is being gained not only into stratospheric dynamics as such, with its implications for pollutant behaviour and the ozone layer, but also indirectly into the dynamics of the troposphere, with its implications for weather forecasting. Similar dynamical regimes occur in the oceans and in stellar interiors. A key development has been the construction of coarse-grain maps of the large-scale distribution of potential vorticity in the middle stratosphere. Potential vorticity is a conservable quantity which has a central role in the dynamical theory, but is difficult to calculate accurately from observational data. We present the first mid-stratospheric potential vorticity maps which appear good enough to make visible the 'breaking' of planetary or Rossby waves, a phenomenon ubiquitous in nature and arguably one of the most important dynamical processes affecting the stratosphere as a whole.

THE flow in the northern wintertime stratosphere is often thought of as consisting of an anticlockwise vortex centred on the cold polar cap, disturbed by a pattern of 'planetary waves'. Two examples are shown in Fig. 1*a*, *b*, which are conventional maps showing the height of the 10-mbar isobaric surface on 17 and 27 January 1979. This surface lies in the middle stratosphere, at heights ranging between about 28 and 32 km. Because there is approximate geostrophic balance between horizontal pressure gradient and Coriolis acceleration, the air flow is nearly parallel to the height contours, as suggested by heavy arrows in Fig. 1. Velocities in the fastest parts of the stream may reach about 75 m s^{-1} (~90° longitude per day at 50° N). The pattern in Fig. 1*a* contains a wave-3 disturbance, consisting of three pairs of ridges and troughs around a latitude circle, while Fig. 1*b* is dominated by a wave-1 disturbance, with a single trough over Europe. This wave-1 disturbance was observed to be nearly stationary with respect to the Earth's surface, and had an unusually large amplitude. It was the first of a sequence of events leading several weeks later to a major sudden warming, during which the circumpolar vortex broke up completely and temperatures in the polar cap rose by tens of degrees in just a few days.

The most prominent wave patterns at these altitudes in winter tend to be more or less stationary and to be dominated by the largest spatial scales, associated with waves 1 and 2 and to a lesser extent with wave 3. As is well known, this fact is in qualitative agreement with the predictions of linear wave theory, if one assumes that the primary source of the waves is in the much denser troposphere below and involves processes tied to large-scale geographical features, favouring the generation of stationary waves. Linear theory predicts that those stationary waves which have the largest horizontal scales penetrate highest.

The dynamical restoring mechanism, whereby the waves can propagate westward relative to the stream and remain stationary on the polar vortex, depends on the existence of a cross-stream gradient of Ertel's potential vorticity in isentropic surfaces. Part of this cross-stream gradient is due to the varying direction of gravity relative to the Earth's rotation axis, the so-called planetary vorticity gradient or 'beta effect', and there are further important contributions dependent on the velocity profile of the airstream. Ertel's potential vorticity Q is defined by

$$Q = \rho^{-1}(2\Omega + \nabla\times\mathbf{u})\cdot\nabla\theta \qquad (1)$$

where Ω is the Earth's angular velocity, $\mathbf{u}$ is air velocity relative to the Earth, ρ is air density and θ specific entropy, the gradient of which is nearly vertical in the stratosphere because the isentropic surfaces are nearly horizontal. One may equally well take θ to be potential temperature, or any other function of specific entropy. The equations of motion imply that, if the motion is adiabatic, that is, if

$$D\theta/Dt = 0 \qquad (2)$$

0028–0836/83/410593–08$01.00

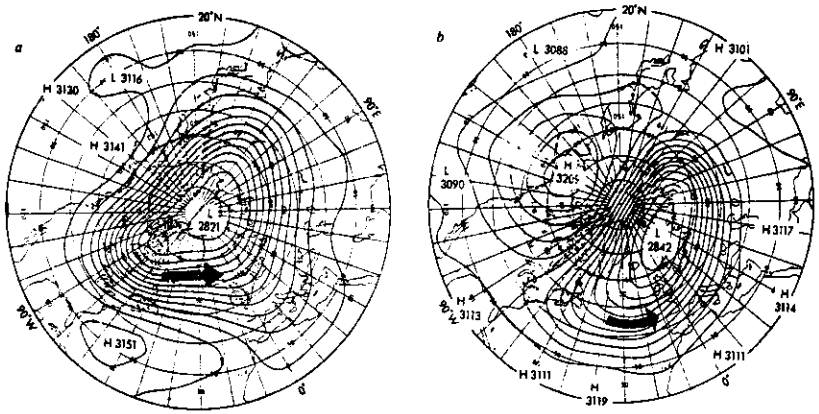

Fig. 1 Geopotential height in decametres (numerically nearly the geometric altitude above sea level) of the 10-mbar isobaric surface on 17 (*a*) and 27 (*b*) January 1979, at 00 h GMT. Contour interval is 24 decametres. Map projection is polar stereographic. The southernmost latitude circle shown is 20° N.

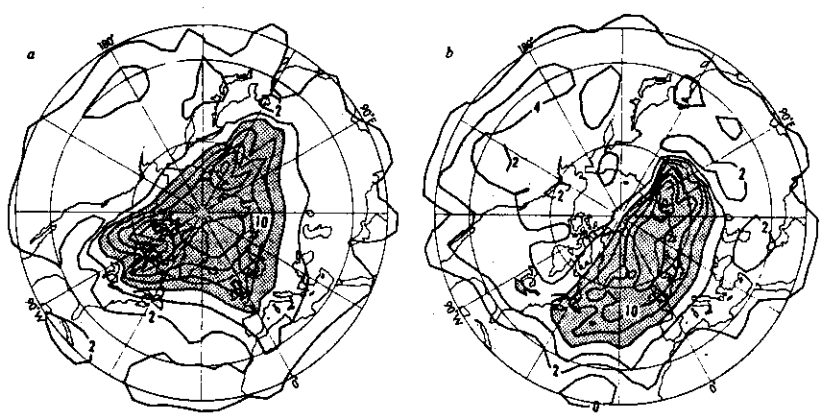

Fig. 2 Coarse-grain estimates of Ertel's potential vorticity Q on the 850 K isentropic surface (near the 10-mbar isobaric surface) on 17 (*a*) and 27 (*b*) January 1979, at 00 h GMT. The southernmost latitude circle shown is 20° N; the others are 30° N and 60° N. Map projection is polar stereographic. For units see equation (5) onwards. Contour interval is 2 units. Values greater than 4 units are lightly shaded, and greater than 6 units heavily shaded.

then, provided also that the motion is frictionless,

$$DQ/Dt = 0 \qquad (3)$$

(Ertel's theorem). $D/Dt = \partial/\partial t + \mathbf{u}\cdot\nabla$ is the rate of change seen by an individual air parcel; thus, Q and θ are constant following the motion. For present purposes this is a qualitatively reasonable approximation, for time scales up to a week or so. Over longer time scales, and in any case for quantitative work, the effects of radiative heating or cooling would have to be included, especially at the highest levels in the stratosphere. Equations (2) and (3) imply that when material contours are displaced northward and southward in a wavy pattern, the contours of potential vorticity in an isentropic surface are similarly displaced. The velocity field associated with the resulting potential vorticity disturbance lags the displacement pattern by a quarter wavelength, implying that the whole pattern propagates westward relative to the stream. This wave propagation mechanism was identified in 1939 by C.-G. Rossby, who recognized its importance for large-scale flow in the troposphere. It is an essentially linear mechanism. Of course, equation (3) itself applies equally well to nonlinear as to linear phenomena. A time sequence of isentropic maps of Q provides not only a good way of seeing when and where the Rossby-wave propagation mechanism is effective (and hence of judging the possible relevance of associated theoretical concepts like group velocity, refractive index, and so on), but also provides a very direct insight into some of the more important consequences of nonlinearity.

Data and approximations

Contour maps of Q on the 850 K isentropic surface in the Northern Hemisphere, at daily intervals during January–February 1979, were constructed at the UK Meteorological Office. 850 K is the potential temperature defined as the temperature of an air parcel brought adiabatically to a nominal sea-level pressure of 1,000 mbar. The data used were 50- and 100-mbar height fields from conventional meteorological objective analyses (NMC, Washington), together with IR spectroscopic radiances from channels 25 and 26 of the prototype Stratospheric Sounding Unit on board the polar orbiting satellite Tiros-N. Channels 25 and 26 receive radiation mainly from the region above 100 mbar, and their weighting functions peak at about 16 and 6 mbar, respectively[1]. The 850 K isentropic surface was chosen because it lies mainly between the peaks of the weighting functions and is one of the most suitable isentropic surfaces, in terms of signal-to-noise ratio, on which to estimate the derivatives required for calculating Q. It is also close to the 10-mbar isobaric surface depicted in Fig. 1, and is centrally placed for observing stratospheric planetary-wave phenomena.

To estimate Q, smoothed height fields on the 20, 10, 5, 2 and 1 mbar isobaric surfaces were derived from the hydrostatic relation and the IR radiances, using standard techniques summarized in Fig. 3 of ref. 1; this is also how the maps in Fig. 1 were obtained. The 1- and 2-mbar fields were inaccurate through failure of the third IR channel, 27, but we believe that this did not materially affect the analysis near 10 mbar. The so-called gradient wind approximation, which assumes geostrophic balance plus a correction allowing for the local curvature of air parcel trajectories, was used to estimate the vertical component ζ of the vorticity vector, $\nabla\times\mathbf{u}$, on each isobaric surface. A simple centred-difference formula having second-order accuracy was used, the height fields having been interpolated onto a square grid on a polar stereographic projection, the grid size being about 580 km at 50° N. The pressure p on the 850 K isentropic surface was then found at each grid point by a cubic spline interpolation procedure, and ζ was similarly interpolated on to that surface. Q was then found from equation (1), taking θ as potential temperature relative to 1,000 mbar and neglecting the small horizontal component of $\nabla\theta$. In estimating the vertical component $\partial\theta/\partial z$ from the data, the hydrostatic relation $\partial p/\partial z = -\rho g$ was again used, giving

$$\rho^{-1}\partial\theta/\partial z = -g\partial\theta/\partial p = -gp^{-1}\partial\theta/\partial(\ln p) \qquad (4)$$

where z is the altitude and g the acceleration due to gravity; $\partial\theta/\partial(\ln p)$ was estimated as the local slope of the curve defined by the appropriate cubic spline. All the vertical interpolations were carried out with respect to $\ln p$, roughly equivalent to using the true altitude z. Further details are given in ref. 2.

It is emphasized that the satellite data can at best represent smeared-out versions of the temperature and motion fields. The horizontal resolution is limited, especially in the tropics, by the number of orbits, about 14 polar orbits per day. The vertical resolution is limited by the half-widths of the weighting functions, just under 10 km. *A fortiori*, the data cannot resolve the fine-grain structure in the θ and Q fields which is to be expected for various reasons, and evidence of which has frequently been seen in the stratosphere, including layers with small vertical scales. Our neglect of the horizontal component of $\nabla\theta$, an approximation valid for large Richardson number, may not apply on the smallest scales either. Fortunately, there are reasons for supposing that the large-scale dynamics 'sees' mainly a coarse-grain, spatially averaged approximation to Q and θ, varying on vertical and horizontal scales not much smaller than those resolvable by the satellite data, and moreover that many of the smaller-scale fluctuations in $\nabla\theta$ and ζ are sufficiently ill-correlated to be ignored, to a first approximation, in a coarse-grain estimate of the right-hand side of equation (1) exploiting the smoothness of the satellite weighting functions. If some such coarse-grain approximation to Q were not dynamically meaningful, numerical model simulations of the large-scale behaviour of the atmosphere would hardly be practicable. The particular stratospheric wave events under discussion were, in fact, remarkably well simulated by a high-resolution numerical forecasting model[3], as far as we can tell from existing diagnostics.

We further caution that all scales are subject to ill-understood systematic errors from the algorithms used to retrieve vertical temperature profiles from IR radiances, and to errors in the radiances themselves[1]. The difficulties in estimating such errors are well known, being partly due to a paucity of independent temperature measurements by other means such as rocket probes in a sufficient variety of conditions. A preliminary assessment of their effects on Q is given in ref. 2. A full investigation is beyond our present resources as it would require the careful intercomparison of all available data, including newly available satellite data on other quasi-conservative tracers such as ozone. This must be left as a major problem for the future, progress with which could eventually lead to improved data exploitation based on simultaneous estimation of the distribution of tracers and potential vorticity.

One of the main points to be made here, however, is that despite the data errors, the present coarse-grain Q maps exhibit certain qualitative features which are strikingly in accordance with expectations from well-explored lines of theoretical reasoning, supported by rational analytical models, by numerical experiments of various kinds, and by direct estimates of relevant material trajectories based on the satellite-derived wind fields. We feel justified, therefore, in claiming that those qualitative features in the Q fields to which we shall draw attention are almost certainly real, and that to this extent the data are dynamically consistent—more so, perhaps, than hitherto appreciated.

This view has received still further support from unpublished maps of another quasi-conservative quantity, ozone mixing ratio, recently obtained from the LIMS limb-scanning satellite radiometer[4]. Daily hemispheric ozone maps on the 10-mbar isobaric surface for the same period were shown to us by Professor C. B. Leovy after a first version of the present paper was circulated to colleagues and submitted for publication. This time sequence of maps shows qualitative features which, within horizontal resolution, strongly support our interpretation of the Q maps. They also provide more information in the tropics, where our estimates of Q are completely unreliable. All we can safely say about the distribution of Q in the tropics is that it must go through zero near the Equator, for reasons of dynamical stability[5,6].

Linear waves versus breaking waves

Two of the 850 K potential vorticity maps are shown in Fig. 2, for 17 and 27 January 1979, the same dates as in Fig. 1. It should be remembered that they are at best coarse-grain maps, that some of the smaller visible features may not be real, and that the real Q fields are likely to have unresolvable fine-grain structure. Owing to data problems in the tropics, details in the outermost contours are especially to be distrusted wherever they extend south of 20° N, the southernmost latitude circle shown. It is probably reasonable to think of the maps as resembling a blurred view of reality seen through a pane of knobbly glass, the size of the knobbles being of the order of many hundreds of kilometres, and more in the subtropics owing to the larger spacing of the satellite orbits there[1,2]. The quantity plotted is

$$\hat{Q} = g^{-1}H_0^{-1}p_0Q \qquad (5)$$

in units of 10^{-4} K m^{-1} s^{-1}, p_0 being a standard sea-level pressure taken as 1,000 mbar and H_0 a standard pressure scale height taken as 6.5 km. Values greater than 6 units are picked out by the heavy shading. To obtain a feel for the numerical values, one may note from equations (1), (4) and (5) that, for a given numerical value of $\hat{Q}$, the vertical absolute vorticity component Z_0 which would be realized if $\partial\theta/\partial p$ were brought to a standard value $\partial\theta_0/\partial p$, by means of an adiabatic, frictionless,

rearrangement of mass, satisfying equations (2) and (3), is given by

$$Z_0 = \frac{-Q}{g\partial\theta_0/\partial p} = \frac{-H_0\hat{Q}}{p_0\partial\theta_0/\partial p} \qquad (6)$$

Conveniently, this equals $0.2\hat{Q}$ in units of 10^{-4} s^{-1}, for example, 2.0×10^{-4} s^{-1} on the contour marked 10 (which may be compared with the maximum planetary vorticity $2\Omega = 1.458\times10^{-4}$ s^{-1}), when $-\partial\theta_0/\partial p$ is taken as 32.5 K mbar^{-1}. The latter value happens to be close to the area average of $-\partial\theta/\partial p$ on the 850 K isentropic surface north of 45° N on 17 January, according to the satellite data analysis scheme, albeit about 15% too high for the 27 January data.

Comparing Fig. 2*a* with Fig. 1*a*, we see that the main circumpolar vortex appears to be a region of substantial cross-stream potential vorticity gradients, suggesting that it is well able to support Rossby-wave propagation. That is no more than has been shown from previous analyses using eulerian averaging around latitude circles, but Fig. 2*a* gives a better idea of the tightness of the gradients and their instantaneous spatial distribution. A large part of the overall gradient between equatorial and polar regions seems to be concentrated near the edge of the heavily shaded region, while systematic poleward gradients are comparatively weak throughout most of the surrounding, unshaded region. It seems unlikely that this structure is a result of radiative heating or cooling, especially when its observed time evolution is taken into consideration (S. B. Fels and D. L. Hartmann, personal communication).

A more likely explanation will emerge from the following discussion, and will suggest in turn that the gradients near the edge of the heavily shaded region may, in reality, be even tighter than they appear on the maps. Taken at face value, as they appear in Fig. 2*a*, the numerical values of these gradients are still quite large. Expressed as isentropic gradients of Z_0 (locally equivalent to isobaric gradients of 'quasi-geostrophic potential vorticity')[7], they reach values exceeding the local planetary vorticity gradient $\beta = 2\Omega a^{-1}\cos\phi$ by well over an order of magnitude, over Canada and eastern Siberia for instance, a being the Earth's radius and ϕ the latitude. The largest contributor is the gradient of ζ. Gradients in $\partial\theta/\partial\ln p$ contribute in the same sense, as does the planetary vorticity gradient itself, but appear to be numerically less important for the coarse-grain Q distribution in the main vortex. (This suggests that the balance of terms discussed by Simmons[8] should give a good first approximation to the wave structure, insofar as it can be described by linear theory.)

Outside the heavily shaded region, there are clear signs that the dynamics is less wave-like, and indeed highly nonlinear. This is suggested particularly strongly by Fig. 2*b*, and also by the Q maps for a number of other days, omitted for brevity. Especially notable is the gross shape of the '4' contour in Fig. 2*b*, picked out by the lighter shading and emphasized in the coloured version on the front cover of this issue. A long tongue of high-Q air seems to have been pulled out from the main vortex, and to be in the process of being mixed quasi-horizontally and irreversibly into the surrounding region of weaker gradients. As we shall see, this can be accounted for in terms of clockwise advection by the large secondary vortex centred north-east of the Aleutian Islands in Fig. 1*b*. Like the rest of the pattern, this Aleutian vortex was nearly stationary in position, although growing in size, during the previous few days. The Aleutian vortex, it appears, was eating its way into the potential vorticity gradient at the edge of the main vortex, systematically reducing the area best capable of supporting Rossby-wave propagation.

Although this erosion of the main vortex, and irreversible mixing of its material into lower latitudes, is a highly nonlinear process, quite outside the scope of linear wave theory, it is familiar from various theoretical model studies. Essentially the same process is illustrated, for instance, by the time-dependent theory of 'nonlinear critical layers'[9,10]. An example is shown in Fig. 3, in which x corresponds to longitude west and $-y$ to

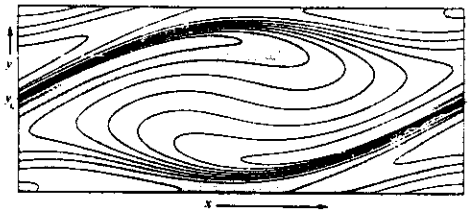

Fig. 3 Analytical solution from the time-dependent theory of nonlinear critical layers[9,10], exhibiting irreversible deformation of material contours due to advection by a two-dimensional (height-independent) 'Aleutian vortex' set up by a stationary Rossby wave on a shear flow. An equation of the form of equation (3) holds exactly, so that the contours are both material contours and contours of Q, or equally its two-dimensional equivalent, the vertical component of absolute vorticity. The shading picks out values of Q intermediate between the higher and lower values (unshaded) at bottom and at top/centre, respectively. The solution is periodic in x. The y scale is exaggerated. Initially the contours lie parallel to the x axis and represent a monotonic gradient of Q. The initial flow is in the x direction before the waves are excited, and its velocity is proportional to $(y - y_c)$ so that there is a 'critical line', where flow speed equals wave phase speed, at $y = y_c$. The time elapsed is 0.57 of the time for an air parcel to make one complete trip around the centre of the vortex or 'cat's eye'.

latitude (see Fig. 3 legend for further detail). This solution was obtained analytically, using the method of matched asymptotic expansions, thus avoiding any questions about numerical resolution. It provides a dynamically consistent model example of the effect of an indefinitely persistent 'Aleutian vortex' on a set of material contours, coinciding with Q contours, which initially lie parallel to the x direction. The model Aleutian vortex is twisting up the contours like spaghetti on a fork, destroying the pre-existing, overall gradient of Q. The shading in Fig. 3 emphasizes the fact that long, thin tongues of material, like that suggested by Fig. 2*b*, are produced by this advective process. The same process has been simulated in various kinds of numerical experiment[10–14]. Figure 3 also illustrates the well known fact that such advective processes tend to produce Q fields of increasingly fine spatial scale, exemplifying the so-called 'potential enstrophy cascade' studied in the theory of geostrophic turbulence[15]. This, of course, is one of the reasons that Q is likely to vary on much finer scales than could possibly be resolved by observational data.

It might still be questioned whether the tongue of high-Q air appearing in Fig. 2*b* is real, since for reasons already indicated there is little hope of showing this directly from the data alone, especially in view of data limitations in the subtropics. Still less is there any point in trying to make direct estimates of the advection term $\mathbf{u}\cdot\nabla Q$ on the left-hand side of equation (3), because the extra differentiation involved in estimating ∇Q would make the effect of small-scale errors even worse than in Q itself. A better check is to use satellite-derived wind fields to calculate isentropic trajectories, which apart from errors in the wind fields would represent the paths of material parcels if equation (2) were exactly satisfied. A number of such trajectories were calculated, integrating backwards in time from a selection of positions within and near the tongue as it appears in Fig. 2*b*. The trajectories were found to extend back around the growing Aleutian vortex to positions close to where the edge of the main vortex had been on the appropriate date. For instance, an air parcel at 177.5° W, 35° N on 27 January, near the tip of the visible tongue, was estimated to have been over the Arctic Ocean about 4 days earlier, around 80° N and close to the 4 contour at the edge of the shaded region. The trajectory crosses the north coast of mainland Canada near Victoria Island before swinging out over the Pacific via northern California. In computing this trajectory we had to correct for the error in the gradient-wind approximation due to strong deceleration of the

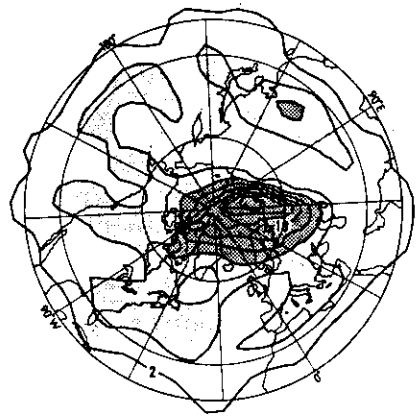

Fig. 4 Ertel's potential vorticity as in Fig. 2, but for 16 February 1979. The shading refers to same contour values as in Fig. 2. The small area of the main vortex suggests that the stratosphere was highly 'preconditioned', that is, susceptible to a major warming.

parcel as it came out of the main vortex[16]. Another air parcel, at 117.5° W, 35° N on 27 January, near Los Angeles, was estimated to have passed close to the North Pole about 2 days earlier, well within the shaded region at the time. Such estimates strongly suggest that advection of high-Q air from the edge of the main vortex could, indeed, have produced a thin tongue having the length, position and gross shape suggested by Fig. 2*b*. They suggest, moreover, that the process would have taken only a few days, so that equations (2) and (3) are likely to have been relevant despite the possible effects of radiative heating or cooling.

The phenomenon seen in Figs 2*b* and 3 is analogous, in a very fundamental sense, to the breaking of ocean waves approaching a beach, and it is appropriate to speak of a breaking Rossby or planetary wave. The basic criterion for saying whether a wave of any kind is breaking is whether material contours and surfaces are being irreversibly deformed, rather than simply undulating back and forth as is assumed in linear wave theory. Wave breaking, in this sense, is undoubtedly a ubiquitous phenomenon and is one of the most effective means whereby waves in naturally occurring flows can cause systematic redistribution not only of potential vorticity, but also of pollutants, angular momentum and other quantities of interest. Other significant examples include (1) the breaking, in the upper troposphere, of packets of Rossby waves radiated upwards and equatorwards by occluding tropospheric depressions[17–19] (vital to the global potential-vorticity and angular momentum balances, but less accessible to direct observation than the present example because the spatial scales are smaller), and (2) the breaking of upward-propagating internal gravity waves in the mesosphere, revealed by noctilucent cloud patterns and by modern radar techniques, and now believed on good evidence to be the key to an old enigma about the global angular momentum balance at altitudes above 50 km (see, for example, ref. 20). Unlike potential vorticity and material tracers, momentum and angular momentum can be transferred between, and not merely within, the sites of wave generation and wave breaking. General theories of wave, mean-flow interaction imply that the distinction between breaking and non-breaking waves—defined, as here, in terms of irreversibility or reversibility of the deformation of material contours—is fundamental to all the aforementioned processes[21]. The distinction seems to be more fundamental, for instance, than questions of detail such as whether local instabilities have any role in deforming the material contours, or whether or not the breaking can be associated with a 'critical layer' as in Fig. 3.

Although the data resolution can hardly be expected to be good enough to reveal wave breaking events of smaller scale than that in Fig. 2*b*, we may note in passing that there is more than a hint of such an event (as seen through 'knobbly glass') in the Z-shaped contour, labelled 2 units, near the bottom of Fig. 2*a*. Despite the severe data problems in this region, the feature is broadly consistent with advection by the observed velocity field during the previous few days. Perhaps more significantly, however, the theoretical considerations mentioned earlier show that the occurrence of such breaking is more or less inevitable in any case, given a few long-accepted observational facts. At most altitudes in the stratosphere, the eulerian-mean flow $\bar{u}$ around latitude circles usually vanishes in at least some part of the tropics or subtropics, as seen in a frame of reference moving longitudinally with the waves of largest amplitude. The waves are often nearly stationary, or moving slowly eastwards (as happens to be the case for the wave-3 disturbance seen in Fig. 1*a*), whereas $\bar{u}$ goes from large eastward values in the winter hemisphere to large westward values in the summer hemisphere. The kinematics of the situation implies the existence of secondary vortices, in the waves' frame of reference, somewhere in the tropics or subtropics, which for realistic wave amplitudes and durations are capable of twisting up material contours irreversibly in the manner illustrated by the analytical solution in Fig. 3.

We therefore conclude (1) that the region of weak potential vorticity gradients surrounding the main vortex is effectively a gigantic 'surf zone', in some part of which planetary waves are breaking most if not all the time, and (2) that the resulting quasi-horizontal mixing is a likely explanation of why the gradients in this zone are observed to be weak.

Encroachment of the surf zone

The analogy between the region surrounding the main stratospheric vortex and the surf zone on an ocean beach appears to be both fundamental and useful, but like any other partial analogy it should not be pushed too far. Two differences may be important. First, theoretical evidence has accumulated suggesting, perhaps surprisingly, that the stratospheric surf zone may be a fairly good Rossby-wave reflector in at least some of the conditions of interest (ref. 11 and refs therein). This is quite unlike an ordinary ocean beach, which is a good wave absorber. Second, whereas ocean beaches are more or less fixed in position, the stratospheric surf zone can encroach polewards whenever erosion of the main vortex is strong enough.

Figure 4, showing Q for 16 February 1979, seems to be an excellent illustration of this last point. The reduction in the heavily shaded area is unmistakable when Fig. 4 is compared with Fig. 2*a*. Indeed, the heavily shaded area in Fig. 4 is perhaps more appropriately compared with the lightly shaded area in Fig. 2*a*, if we define the area of the main vortex by reference to the outer edge of the region of tight gradients. We consider erosion due to wave breaking to be the most plausible explanation. It can simultaneously explain the reduction in the area of the main vortex, the corresponding broadening of the surrounding zone of weak gradients, and the persistently tight gradients marking the interface between them (apparent in all the available Q maps for the period). Gradients as tight as this, or even tighter, are characteristic of the sharp interface between a well mixed and a less mixed region when there is an overall gradient of some quasi-conservable quantity across the two regions. The phenomenon is familiar in several contexts, and has often been demonstrated in small-scale laboratory experiments[22]. The idea that vigorous quasi-horizontal mixing was occurring outside the main vortex seems consistent not only with Figs 1*b* and 2*b* but also with the entire sequence of daily Q maps for late January and early February. Most of these maps show clear signs of large-amplitude wave breaking, on a scale which seems ample to account for the observed broadening and encroachment of what we have called the surf zone.

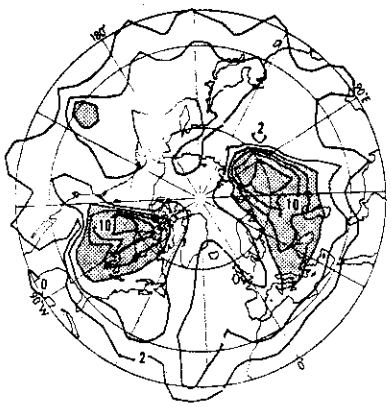

Fig. 5 Ertel's potential vorticity as in Fig. 2, but for 23 February 1979, showing the effect of the subsequent major warming.

Additional supporting evidence comes from the LIMS ozone maps shown to us by Professor Leovy. They show what seems to be the same main-vortex, surf-zone structure, evolving in time in the same way. Erosion by wave breaking can easily explain this structure and evolution because, like Q, the ozone mixing ratio is a quasi-conservative quantity in the middle stratosphere, approximately satisfying an equation of the form of equation (3) over time scales of the order of days. Alternative explanations in terms of diabatic or photochemical effects seem less likely to be successful because, although such processes cannot be expected to be negligible over the whole period in question, there is no obvious reason that they should affect ozone in the same way as Q.

Resonance, preconditioning, sudden warmings

The abovementioned differences between the stratospheric surf zone and an ordinary beach may be significant for various reasons, one of which is the much-discussed possibility[11] that the main vortex may behave like a resonant cavity. If so, changes in its area induced by wave breaking could provide a robust and effective mechanism for the nonlinear self-tuning or detuning of the cavity. In a recent theoretical study, Plumb[23] has pointed out that an approach to resonance via nonlinear self-tuning (that is, 'topographic instability')[24] can explain not only the growth of stationary wave-1 amplitude, but also the simultaneous slowing down of a weaker, westward-travelling wave-1 component in the height field, such as was observed to precede the large-amplitude wave-1 event of Fig. 1*b*[25,26]. Whilst the idea of a self-tuning resonant cavity fits closely with such observations, other explanations of the apparent travelling-wave behaviour are also possible, and the very interesting theoretical questions thus raised have yet to be settled definitively.

Another significant aspect is the 'preconditioning' of the stratosphere to make it susceptible to the occurrence of a major sudden warming. From the present viewpoint, it seems natural to regard major warmings as wave events which break up the main vortex completely, advecting low potential vorticity air over the Pole along with ozone and other tracers. The accompanying descent of air parcels, due to the adjustments which maintain approximate geostrophic and hydrostatic balance, causes adiabatic compression, and hence the large polar temperature rises giving such events their customary name. This notion of a major warming as involving complete breakdown of the main vortex does not quite coincide with the definition currently adopted by the World Meteorological Organization, but seems closer to dynamical fundamentals and is consistent, moreover, with views long held by some synoptic meteorologists[27]. The idea that some kind of preconditioning process precedes a major warming goes back to the remarks by Quiroz, Miller and Nagatani in 1975 (see, for example, ref. 11 and refs therein), and it is now widely believed that such an idea is needed to explain many of the observed facts, including the fact that major warmings do not occur more often.

Preconditioning has often been thought of in terms of changes in the eulerian-mean state of the stratosphere, defined by taking averages around latitude circles. But it now seems evident that a much more fundamental and practically useful measure of preconditioning would be in terms of the reduction in the area of the main polar vortex, or degree of encroachment of the stratospheric surf zone. The advantage of fixing attention on the area of the main vortex is that it eliminates from consideration the large but purely temporary dynamical effects, on the eulerian mean at high latitudes, of transient, reversible disturbances to the main vortex, such as bodily migrations towards or away from the pole accompanied by little or no wave breaking. Instead, it fixes attention on the more permanent, irreversible dynamical effects, in which potential vorticity is being drastically rearranged rather than simply being moved back and forth.

We predict that unusually small values of the area A of the main vortex, as it appears on daily stratospheric potential-vorticity maps, will be found to be characteristic of the conditions observed just before major warmings. The smaller the value of A, the smaller the region best capable of supporting Rossby-wave propagation. Small values of A may thus give rise to a focusing effect, tending to concentrate any subsequent wave disturbance into a smaller and less massive region than usual (a linear model of the disturbance structure again involving Simmons' approximate balance of terms[8]). Evidence suggesting the importance of this focusing effect in the events leading to a major warming can be found both in the observational data and in numerical simulations[11]. An objective definition of A which could be used to investigate its day-by-day behaviour is proposed in ref. 16.

Experiment in stratospheric dynamics

When the area of the main vortex is as small as Fig. 4 suggests it was on 16 February 1979, the preconditioning process is far advanced, according to our hypothesis, and a subsequent major warming very likely. In this case a major warming did occur, several days later. This warming was of exceptional interest for two reasons. The first was that the wave event precipitating it appeared to be unusually simple in form, with wave 2 dominating the eddy fluxes which measure the upward propagation of wave activity from the troposphere. Very large wave-2 amplitudes developed, splitting the main vortex cleanly in half in the course of a few days. The resulting coarse-grain potential vorticity distribution is indicated in Fig. 5, the map for 23 February. The unusual weakness of wave 1 during the splitting process provided direct evidence that large wave-1 amplitudes are not essential to that process[21].

The second reason that this particular warming was especially interesting was the fact that it did not occur sooner. On the basis of past case studies, one might well have expected a major warming to have occurred by mid-February[25]. In this case, however, the preconditioning process was unusually well separated in time from the warming itself. These circumstances, the lateness of the warming and the unusually simple wave structure when it did occur, combined to make it one of the most useful 'controlled experiments' in stratospheric dynamics ever performed by the real atmosphere. This has already been taken advantage of in computer simulations which have successfully 'repeated' the experiment, and also varied its conditions in several different ways[3,28]. The possibilities of such numerical experiments are still far from being exhausted.

Most of the other major warmings observed during the past two decades involved large-amplitude, complicated-looking

mixtures of waves 1, 2 and higher. However, drawing on what has been learned from the case of January–February 1979, we may anticipate that much of this apparent complexity will disappear as soon as attention is focused on the main vortex as the dynamical centre of things, rather than on any analysis tied to latitude circles, such as the conventional Fourier analysis of the height and temperature fields into separate wavenumbers. For instance, in the celebrated major warming of January 1977, the main vortex split in much the same way as in February 1979, the only difference being that it happened to be displaced well away from the Pole at the time, over Baffin Island[29]. Only the Fourier analysis was complicated, not, it seems, the physical phenomenon. Regarded as a wave-2 disturbance relative to the displaced main vortex[30], rather than relative to latitude circles, the observed phenomenon appears remarkably similar to that of February 1979. Indeed, the whole sequence of events leading to the warming, and no doubt those leading to other major warmings, can probably be viewed in essentially the same simple way as above, the main difference being that the preconditioning process (erosion of the main vortex) may not be well separated in time from the subsequent major warming. We await with interest the potential vorticity maps which will help to confirm or disprove these suggestions.

Conclusion

Our understanding of large-scale dynamical and eddy transport processes in the atmosphere would be greatly improved if daily isentropic maps of Ertel's potential vorticity Q were to become available on a routine basis. For example, they would increase our ability to judge the relevance of numerical model experiments and of theoretical concepts such as 'wave propagation', 'instability', 'critical layers' and so on. The above examples from the middle stratosphere seem sufficient to show that the effort would be worthwhile, despite the impossibility of resolving the finest scales in the potential vorticity patterns.

The coarse-grain Q maps presented here used nothing more than standard data-processing techniques applied to routinely-available meteorological data, but besides sharpening our insights into stratospheric dynamics in general, they have already suggested some specific, testable hypotheses. One such hypothesis is that large-scale wave breaking, leading to erosion of the main circumpolar vortex, will be found to be characteristic of the circumstances leading to major stratospheric warmings. The existence of long, thin tongues of material coming off the edge of the main vortex, a process which we believe we are seeing for the first time in Fig. 2*b* albeit in a blurred and distorted form, may soon be independently verifiable in this and other cases by means of data now becoming available from the newest satellite radiometers. An additional check may come from Q maps and air-parcel trajectories derived from high-resolution numerical simulations. For instance, the latest numerical forecasting models have far better horizontal resolution than data from polar-orbiting satellites, and should be able to represent a feature like the long tongue in Fig. 2*b* in considerable detail.

The prediction that A, the area of the main vortex on a given day, will be found to decrease systematically during the buildup to a major warming, should be testable even with data whose horizontal resolution is too coarse to show wave-breaking details. For this purpose the only demand on the data is that an objective measure of A be feasible[16], based on the anticipated tightness of isentropic gradients of Q near the edge of the main vortex. If time series of daily values of A, on some convenient isentropic surface, could be obtained from long, homogeneous runs of data, then other possibilities would be opened up. Such time series should be very effective as indicators of the general state of the stratosphere during a succession of winters. They represent a good combination of simplicity and finesse, since the use of daily estimates of A avoids the loss of information incurred by taking eulerian space or time means. Time series of A might substantially aid current attempts to correlate the interannual variability of the winter stratosphere with other long-term variations such as the quasi-biennial oscillation in the tropical stratosphere, or El Niño and the Southern Oscillation in the troposphere.

Assuming that our findings are confirmed, they also have implications for the next generation of stratospheric tracer transport models, with which the possible effects of pollutants on the ozone layer will be studied. Short of attempting to simulate the three-dimensional motion of the entire troposphere, stratosphere and above[31], some success has already been achieved with 'two-dimensional' models in which the material transports are represented by means of eulerian eddy fluxes relative to latitude circles. A number of significant suggestions for improving models of this kind have recently been made[32–36], and the observational picture now emerging should be a useful input to such modelling efforts. Indeed, it suggests that the most efficient two-dimensional modelling strategy might, in fact, be to abandon altogether the description tied to latitude circles, and instead to partition each isentropic layer in the stratosphere into several regions on the basis of the coarse-grain distribution of Q—say, a main vortex, a surrounding surf zone, and other regions representing the tropics and the summer hemisphere. From a theoretical point of view, this would amount to a low-resolution 'modified lagrangian-mean description'[37] of the stratosphere. The mass of each region would change with time according to observational estimates of erosion rates, in competition with the rate of replenishment of potential vorticity by diabatic processes such as IR cooling in the polar night. The detailed implementation of such a model has yet to be worked out.

For the troposphere, the best hope of obtaining the needed Q maps may be to use dynamically consistent 'data' derived from high-resolution numerical weather forecasting models and analysis schemes, rather than making any attempt to use raw observational data. We may anticipate that Q maps produced as part of the daily numerical forecasting operation will prove valuable in the routine assessment of the forecasts themselves, since they make the model dynamics highly visible. For instance, evidence now becoming available suggests that such maps will lead to immediate insights into the formation and maintenance of the mid-latitude 'blocking' situations which lead to anomalous spells of weather (B. J. Hoskins, G. J. Shutts, personal communication; see also refs 38, 39). They would also make it easier to see what dynamical instability mechanisms are likely to be operating in a given locality. Another promising area concerns the interaction between middle latitudes and the subtropics, one aspect of which is the reflectivity of the subtropics to the packets of Rossby waves radiated upwards and equatorwards by occluding mid-latitude depressions[17–19]. The theory of nonlinear critical layers suggests that this reflectivity, whose effects could be important for medium-range weather forecasting, will be dependent from day to day on the distribution of Q on isentropic surfaces in the high troposphere equatorward of the subtropical jet, where the waves may be expected to break.

A longer version of this article, with more figures and a more complete bibliography, is to appear as ref. 16. An extensive bibliography and background discussion may also be found in a recent review article by one of us[11].

We thank S. A. Clough and N. S. Grahame for generous help with the estimation of Q, P. D. Killworth and J. Venn for producing Fig. 3, J. Austin for valuable assistance with some of the isentropic trajectory calculations, C. B. Leovy for his kindness in showing us the unpublished LIMS ozone maps, also D. G. Andrews, S. A. Clough, S. B. Fels, D. L. Hartmann, P. H. Haynes, E. O. Holopainen, J. R. Holton, B. J. Hoskins, C. P. F. Hsu, K. Labitzke, R. S. Lindzen, J. D. Mahlman, R. McIntyre, A. O'Neill, D. R. Pick, R. S. Quiroz, P. B. Rhines, G. J. Shutts and A. F. Tuck for useful discussions or correspondence. The data were kindly supplied by the Met. O. 20 stratospheric analysis team.

Note added in proof: For related work on large-scale ocean dynamics, see ref. 40.

Received 20 April; accepted 18 August 1983.

1. Pick, D. R. & Brownscombe, J. L. *Adv. Space Res.* **1**, 247–260 (1981).
2. Grisham, N. S. & Clough, S. A. Met. O. 20 Tech. Note, available from U.K. Meteorological Office (1983).
3. Simmons, A. J. & Ströfing, R. *Q. J. met. Soc.* **109**, 81–111 (1982).
4. Gille, J. C. & Russell, J. M. *J. geophys. Res.* (submitted).
5. Dunkerton, T. J. *J. atmos. Sci.* **38**, 2354–2364 (1981).
6. Stevens D. E. *J. atmos. Sci.* **40**, 882–893 (1983).
7. Charney, J. G. & Stern, M. E. *J. atmos. Sci.* **19**, 159–172 (1962) [see Eq. (2.31)].
8. Simmons, A. J. *Q. Jl R. met. Soc.* **100**, 76–108 (1974).
9. Stewartson, K. *Geophys. Astrophys. Fluid Dyn.* **9**, 185–200 (1978).
10. Warn, T. & Warn, H. *Stud. appl. Math.* **59**, 37–71 (1978).
11. McIntyre, M. E. *Jl met. Soc. Jap.* **60**, 37–65 (1982).
12. Hsu, C.-P. F. *J. atmos. Sci.* **38**, 189–214 (1981).
13. Matsuno, T. *Proc. US–Japan Seminar on the Dynamics of the Middle Atmosphere* (eds Holton, J. R. & Matsuno, T., Terrapub, Tokyo (in the press).
14. Allam, R. J. & Tuck, A. F. *Q. Jl R. met. Soc.* (submitted).
15. Rhines, P. B. *A. Rev. Fluid Mech.* **11**, 401–441 (1979).
16. McIntyre, M. E. & Palmer, T. N. *J. atmos. terr. Phys.* (in the press).
17. Gill, A. E. *Atmosphere-Ocean Dynamics*, 13.9 (Academic, New York. 1982).
18. Edmon, H. J. *et al. J. atmos. Sci.* **37**, 2600–2616 (1980) (corrigendum **38**, 1115, 1981).
19. Hoskins, B. J. in *Large-scale Dynamical Processes in the Atmosphere* (eds Hoskins, B. J. & Pearce, R. P.) 169–199 (Academic, New York. 1983).
20. Holton, J. R. *J. atmos. Sci.* **39**, 791–799 (1982).
21. Andrews, D. G. & McIntyre, M. E. *J. Fluid Mech.* **89**, 609–646 (1978).
22. Turner, J. S. *Buoyancy Effects in Fluids*, 9.1.1. (Cambridge University Press, 1973).
23. Plumb, R. A. *J. atmos. Sci.* **38**, 2514–2531 (1981).
24. Charney, J. G. & DeVore, J. G. *J. atmos. Sci.* **36**, 1205–1216 (1979).
25. Labitzke, K. *Beilage zur Berliner Wetterkarte*, SO 10/79 (Institut für Meteorologie der Freien Universität Berlin, 1979).
26. Madden, R. A. & Labitzke, K. *J. geophys. Res.* **86C**, 1247–1254 (1981).
27. Labitzke, K. *Mon. Weath. Rev.* **105**, 762–770 (1977).
28. Butchart, N. *et al. Q. Jl R. met. Soc.* **108**, 475–502 (1982).
29. O'Neill, A. & Taylor, B. F. *Q. Jl R. met. Soc.* **105**, 71–92 (1979).
30. Palmer, T. N. & Hsu, C.-P. F. *J. atmos. Sci.* **40**, 909–928 (1983).
31. Fels, S. B. *et al. J. atmos. Sci.* **37**, 2265–2297 (1980).
32. Harwood, R. S. *Phil. Trans. R. Soc.* **A296**, 103–127 (1980).
33. Matsuno, T. *Pure appl. Geophys.* **118**, 189–216 (1980).
34. Danielsen, E. F. *J. atmos. Sci.* **38**, 1319–1339 (1981).
35. Holton, J. R. *J. geophys. Res.* **86C**, 11989–11994 (1981).
36. Tung, K. K. *J. atmos. Sci.* **39**, 2330–2355 (1982).
37. McIntyre, M. E. *Phil. Trans. R. Soc.* **A296**, 129–148 (1980).
38. Shutts, G. J. *Q. Jl R. met. Soc.* (in the press).
39. Illari, L. & Marshall, J. C. *J. atmos. Sci.* (in the press).
40. Holland, W. R., Keffer, T. & Rhines, P. B. *Nature* (submitted).

Inhibition of RNA cleavage but not polyadenylation by a point mutation in mRNA 3′ consensus sequence AAUAAA

Craig Montell*, Eric F. Fisher†, Marvin H. Caruthers† & Arnold J. Berk*

* Department of Microbiology and Molecular Biology Institute, University of California, Los Angeles, California 90024, USA
† Department of Chemistry, University of Colorado, Campus Box 215, Boulder, Colorado 80309, USA

A single U→G transversion in the 3′ consensus sequence AAUAAA of the adenovirus early region 1A gene was constructed and the effect of this mutation on processing of the 3′ end of the nuclear early region 1A RNAs was analysed. The results demonstrate that the intact AAUAAA is not required for RNA polyadenylation but is required for the cleavage step preceding polyadenylation to occur efficiently.

THE AAUAAA hexanucleotide and closely related sequences are the only primary structures common to the 3′ ends of mRNAs in higher eukaryotes, excluding histone mRNAs[1]. Because most non-histone mRNAs are polyadenylated, this observation led to the suggestion[1,2] that AAUAAA is part of a recognition signal required for proper processing and polyadenylation of eukaryotic mRNAs. This was confirmed by Fitzgerald and Shenk[3], who showed that in a Simian virus 40 (SV40) mutant, deletion of the entire AAUAAA sequence shifted polyadenylation to just downstream from the next most proximal AAUAAA. The mechanism of polyadenylation in higher eukaryotes has not been established. However, it has been shown that in the synthesis of papovavirus[4–7], adenovirus[8–14] and several cellular mRNAs[15–18], transcription proceeds beyond the polyadenylation site of the mature message. An endonucleolytic cleavage probably occurs in these primary transcripts at the site of polyadenylation to generate a substrate for a poly(A) polymerase which polymerizes adenylate residues onto the 3′ hydroxyl group of polynucleotides[13,14,17–21]. To explore the function of the AAUAAA sequence in the RNA cleavage and polyadenylation steps, we constructed a point mutation in this hexanucleotide in an adenovirus 2 (Ad2) transcription unit, E1A and analysed the effects of the mutation on processing of the 3′ ends of E1A nuclear transcripts.

The mRNAs synthesized from early region 1A (E1A) of adenovirus 2 are typical of mRNAs in higher eukaryotes; they are spliced[22–24], and contain a 5′-terminal cap[25], noncoding regions at both the 5′ and 3′ ends and a poly(A) tail[26]. Figure 1 shows the sequence of the distal portion of the 3′-untranslated sequence encompassing the AAUAAA sequence and extending to the previously reported polyadenylation site near nucleotide 1,630 (ref. 26). Although some variants of this hexanucleotide have been reported[27–30], the U in the third position seems to be completely conserved. Therefore, we constructed an adenovirus mutant having a T→G transversion at this position in the DNA sequence.

RNA cleavage and polyadenylation

The T in the third position of the adenovirus E1A AATAAA sequence was changed to a G by oligonucleotide-directed mutagenesis of an M13·E1A clone[31–34]. The mutation was transferred into the adenovirus genome[35] to generate a mutant virus designated Ad2pm1610 (pm1610 = point mutation at nucleotide 1,610 in the Ad2 sequence[36]).

To analyse the effect of the point mutation on the processing of the 3′ ends of the E1A nuclear RNAs (nRNAs), we prepared nRNA from HeLa cells[11] infected with either wild-type Ad2 or Ad2pm1610. Total nRNA was fractionated into poly(A)$^+$ and poly(A)$^-$ RNA (that is, poly(A) tails shorter than 15 residues) by repeated passages over oligo(dT)–cellulose columns[37] and then analysed by the hybridization/S_1 nuclease method[38]. In this technique the RNA is hybridized to ^{32}P-labelled DNA probes in DNA excess, digested with S_1 nuclease to hydrolyse the single-stranded RNA and DNA and the S_1-protected RNA/DNA hybrid fragments are denatured and fractionated on polyacrylamide gels. As the hybridizations are performed in DNA excess and proceed to near completion, the intensities of the S_1-protected bands seen in the autoradiograms are a measure of the concentration of RNA in the analyses.

Figure 2*a* shows the S_1-protected fragments resulting from hybridization of the Ad2 E1A nRNAs to a DNA probe 3′ end labelled with ^{32}P at 1,337 in the Ad2 sequence. This probe (probe A, Fig. 2*d*) is labelled near the 3′ end of E1A and continues past the E1A polyadenylation site to include the 5′ end of the next transcription unit, E1B. The major 290-nucleotide band seen in the analysis of Ad2 nRNA is protected by the

0028-0836/83/410600—06$01.00

Properties of the Eliassen-Palm Flux for Planetary Scale Motions[1]

T. N. PALMER[2]

Department of Atmospheric Sciences, University of Washington, Seattle 98195

(Manuscript received 3 November 1981, in final form 3 February 1981)

ABSTRACT

Properties of the quasi-geostrophic Eliassen-Palm (EP) flux for planetary scale motions are discussed, in order to clarify how these properties generalize from their beta-plane counterparts when no restriction on the variation of the Coriolis parameter is imposed. These properties include the relationships between the divergence of the EP flux and the meridional flux of potential vorticity, and between the EP flux, group velocity and refractive index.

1. Introduction

Use of the Eliassen-Palm (EP) flux as a diagnostic both of wave propagation and wave, mean-flow interaction has been made by a number of authors (see, e.g., Dunkerton *et al.*, 1981; Edmon *et al.*, 1980; Palmer, 1981a). While many of the properties of the quasi-geostrophic EP flux are straightforwardly and unambiguously defined on a beta plane (see Edmon *et al.*, 1980), a number of possible ambiguities have appeared in the literature when it is necessary to consider the variation $\Delta(\ln f)$ of the Coriolis parameter over some path segment of an EP flux trajectory. For planetary-scale motions these trajectories are observed to extend over a considerable region of the meridional plane, from high to low latitudes (see, e.g., Palmer, 1981a); hence such variation may be somewhat larger than a typical Rossby number.

In this paper we consider some of the properties of the EP flux for these scales of motion, in particular the relation between the EP flux divergence and the meridional flux of eddy potential vorticity, and the relations between the EP flux, group velocity and the zonal mean refractive index in the WKBJ limit. This latter diagnostic has appeared in a number of different forms (e.g., Butchart *et al.*, 1982; Karoly and Hoskins, 1982; and O'Neill and Youngblut, 1982) as that quantity whose gradient determines the refraction of group velocity paths or EP flux trajectories, and it is clearly of interest to ascertain which, if any, of these forms holds for planetary scale motions. In this paper a planetary-scale motion is formally defined to be one for which Burger's (1958) quasigeostrophic theory is appropriate. In this theory $\Delta(\ln f)$ is taken to be O(1).

It is found that all the beta-plane results can be carried over though a number of subtleties arise. Firstly, with the usual form for eddy potential vorticity on the sphere (e.g., as defined in Edmon *et al.*, 1980), the meridional flux of eddy potential vorticity is not proportional to the EP flux divergence, in the geostrophic approximation. However, a modified potential vorticity can be defined with the property that its meridional flux is equal to the form of the EP flux divergence as it appears in the zonal mean momentum equation. The resulting eddy potential vorticity equation is identical to that given by Matsuno (1970, 1971).

Secondly, the quantity that exactly describes the refraction of either group velocity paths or EP flux trajectories for planetary-scale motion is Matsuno's index of refraction squared divided by the sine of latitude squared. A consequence of this form of refractive index is that in low latitudes, EP flux trajectories should have little or no vertical component, even if the zonal mean wind is locally westerly.

Furthermore, the equation that expresses the refraction of the EP flux trajectories in the WKBJ limit cannot easily be written in a coordinate invariant form and there is a unique coordinate grid in the meridional plane (which differs from a latitude, height grid) on which EP flux trajectories are straight lines in the absence of a gradient in refractive index. One consequence of this is that on a standard latitude, height grid it is possible for EP flux trajectories to look curved yet not be refracted. In practice this coordinate distortion is not important because, in general, refraction effects will be dominant.

[1] Contribution No. 618, Department of Atmospheric Sciences, University of Washington, Seattle.

[2] Permanent affiliation: Meteorological Office, Bracknell, Berkshire, England.

0022-4928/82/050992-06$05.50

52

2. EP flux divergence and potential vorticity flux

With beta-plane geometry, the quasi-geostrophic EP flux, **F**, is given in the $(y$–$z)$ plane by

$$\mathbf{F} = e^{-z/H}\left(-\overline{u'v'},\ f_0\frac{\overline{v'\theta'}}{\bar{\theta}_z}\right).$$

Overbars and primes denote zonal means and departures from zonal means. The coordinate y represents northward distance, and z denotes a log-pressure coordinate with constant scale height H. Zonal and meridional velocity are given by u and v, f is the Coriolis parameter, equal here to a constant mid-latitude value f_0, and θ is potential temperature. Static stability is given by $\bar{\theta}_z$ where subscripts x, y or z denote partial differentiation with respect to x, y or z.

Defining the quasi-geostrophic eddy potential vorticity flux on the beta plane as

$$q'_{(\beta)} = v'_x - u'_y + f_0\left(\frac{\theta'}{\bar{\theta}_z}e^{-z/H}\right)_z e^{z/H}, \qquad (2.1)$$

then

$$\overline{v'q'_{(\beta)}}$$

$$= -(\overline{u'v'})_y + \overline{u'v'}_y + \left(f_0\frac{\overline{v'\theta'}}{\bar{\theta}_z}e^{-z/H}\right)_z e^{z/H} - \frac{f_0}{\bar{\theta}_z}\overline{\theta'v'}_z$$

$$= \nabla\cdot\mathbf{F}\,e^{z/H},$$

since on a beta plane the geostrophic wind is non-divergent, and, from the thermal wind relationship, $v'_z \propto \theta'_x$. Here x is the zonal coordinate.

In spherical geometry the EP flux becomes

$$\mathbf{F} = r\cos\phi e^{-z/H}\left(-\overline{u'v'},\ f\frac{\overline{v'\theta'}}{\bar{\theta}_z}\right), \qquad (2.2)$$

where r is the radius of the earth and ϕ is latitude. With eddy potential vorticity on the sphere defined (as in Edmon *et al.*, 1980) by replacing Cartesian derivatives with spherical derivatives in (2.1), then

$$q' = v'_x - \frac{1}{\cos\phi}(\cos\phi u')_y + f\left(\frac{\theta'}{\bar{\theta}_z}e^{-z/H}\right)_z e^{z/H}, \qquad (2.3)$$

where

$$\frac{\partial}{\partial x} = \frac{1}{r\cos\phi}\frac{\partial}{\partial\lambda},$$

$$\frac{\partial}{\partial y} = \frac{1}{r}\frac{\partial}{\partial\phi},$$

and λ is longitude. Substituting for the geostrophic wind in (2.3), then for planetary-scale motions $\overline{v'q'}$ is no longer proportional to the EP flux divergence. The reason for this is simply the fact that for such scales the geostrophic wind is horizontally divergent.

If, on the other hand, a quantity $q'_{(M)}$ is defined by

$$q'_{(M)} = v'_x - \frac{f}{\cos\phi}\left(\frac{\cos\phi}{f}u'\right)_y + f\left(\frac{\theta'}{\bar{\theta}_z}e^{-z/H}\right)_z e^{z/H}, \qquad (2.4)$$

then

$$\overline{v'q'_{(M)}} = -\frac{1}{\cos^2\phi}(\cos^2\phi\overline{u'v'})_y + \frac{\overline{(\cos\phi fv')_y u'}}{(\cos\phi f)} + \left(f\frac{\overline{v'\theta'}}{\bar{\theta}_z}e^{-z/H}\right)_z e^{z/H} - \frac{f}{\bar{\theta}_z}\overline{\theta'v'}_z,$$

$$= \nabla\cdot\mathbf{F}/(r\cos\phi e^{-z/H}) \qquad (2.5)$$

since $(\cos\phi fv')_y = -\cos\phi fu'_z$ for the geostrophic wind, and the thermal wind relationship $v'_z \propto \theta'_x$ still holds. The quantity on the right-hand side of (2.5) is simply the total eddy-induced forcing on the zonal mean circulation as given by the transformed Eulerian-mean zonal momentum equation in log-pressure coordinates (see Palmer, 1981a)

$$\frac{\partial\bar{u}}{\partial t} - f\bar{v}^* = \nabla\cdot\mathbf{F}/(r\cos\phi e^{-z/H}).$$

Here $\bar{v}^*$ is the meridional component of the residual circulation (see Edmon *et al.*, 1980).

The quantity $q'_{(M)}$ can be considered as a modified potential vorticity since the equation

$$\left(\frac{\partial}{\partial t} + \bar{u}\frac{\partial}{\partial x}\right)q'_{(M)} + \bar{q}_y v' = 0, \qquad (2.6)$$

with

$$\bar{q}_y = \frac{2\Omega\cos\phi}{r} - \left\{\frac{1}{\cos\phi}(\bar{u}\cos\phi)_y\right\}_y + f\left(\frac{\bar{\theta}_z}{\bar{\theta}_z}e^{-z/H}\right)_z e^{z/H},$$

is identical to the linearized potential vorticity equation used by Matsuno (1970, 1971) for studying both planetary-wave propagation and the interaction of planetary waves with a zonal mean flow. The difference between $q'_{(M)}$ and q' is equal to $u'd\ln f/dy$, and arises because the meridional component of wind which advects planetary vorticity must, by scaling arguments, include not only the geostrophic wind, but also the isallobaric component

$$v'_i = \frac{1}{f}\left(\frac{\partial}{\partial t} + \bar{u}\frac{\partial}{\partial x}\right)u'$$

(see Matsuno, 1970, Section 2; and Matsuno, 1971, Section 3a, for details). Hence

$$\left(\frac{\partial}{\partial t} + \bar{u}\frac{\partial}{\partial x}\right)q'_{(M)} = \left(\frac{\partial}{\partial t} + \bar{u}\frac{\partial}{\partial x}\right)q' + v'_i\frac{df}{dy}.$$

Matsuno argued that the form (2.6) was necessary to be consistent with Lorenz's (1960) arguments on

53

the energetics of approximate systems of equations. Equivalently, if (2.6) is multiplied by $q'_{(M)}$ and zonally averaged, then for linear conservative waves on a steady zonal flow we have the local conservation equation

$$\partial A_{(M)}/\partial t + \nabla \cdot \mathbf{F} = 0, \tag{2.7}$$

where

$$A_{(M)} = \frac{1}{2} r\cos\phi e^{-z/H}\overline{q'^2_{(M)}}/\bar{q}_y . \tag{2.8}$$

is an exactly conservable measure of local quasi-geostrophic planetary scale activity. In contrast, the quantity

$$A = \frac{1}{2} r\cos\phi e^{-z/H}\overline{q'^2}/\bar{q}_y ,$$

is only an approximate conservable density. Following the nomenclature of Edmon *et al.* (1980), $A_{(M)}$ may be referred to as the density of EP planetary scale wave activity.

Finally, we may define a velocity

$$\mathbf{C}_{(M)} = \mathbf{F}/A_{(M)} \tag{2.9}$$

which, from (2.7), advects linear conservative EP planetary scale wave activity in the meridional plane.

3. EP flux and group velocity

Consider a steady wave with zonal wavenumber k, frequency ω, and geopotential Φ. If ψ is defined by

$$\Phi = e^{z/2H}\,\mathrm{Re}\{\psi e^{i(kx-\omega t)}\},$$

then (2.6) can be written as the second-order differential equation

$$\left(\omega - \frac{\bar{u}k}{r\cos\phi}\right)\left\{\mu^2\frac{\partial^2\psi}{\partial Y^2} - \frac{k^2}{r^2\cos^2\phi}\psi + \frac{f^2}{N^2}\left|\nu^2\frac{\partial^2\psi}{\partial Z^2} - \frac{1}{4H^2}\psi\right|\right\} - \frac{k\bar{q}_y}{r\cos\phi}\psi = 0, \tag{3.1}$$

where $N^2 = N^2(z)$ is the Brunt-Vaisalla frequency,

$$\mu = \sin^2\phi/\cos\phi, \quad \nu = (N/\Omega)^2,$$

Ω is an arbitrary normalizing constant, and Y and Z are coordinates defined by the transformations

$$dY = \mu dy, \quad dZ = \nu dz,$$

which are introduced so that no first-order derivatives occur in (3.1). Putting

$$\psi = |\psi|e^{i\zeta}, \tag{3.2}$$

we can obtain locally wavelike (or WKBJ) solutions to (3.1) in the form

$$\zeta = lY + mZ, \tag{3.3}$$

where $|\psi|$, l and m are slowly varying functions (see below).

The dispersion relation for such a solution is, from (3.1),

$$\omega = \left(\frac{\bar{u}k}{r\cos\phi} - \frac{k\bar{q}_y}{r\cos\phi}\right)\Big/ \left\{\mu^2 l^2 + \frac{f^2}{N^2}\nu^2 m^2 + \frac{k^2}{r^2\cos^2\phi} + \frac{f^2}{4H^2N^2}\right\}, \tag{3.4}$$

The components of group velocity in the meridional plane are defined in the (Y, Z) coordinate system by

$$C_{(g)}{}^Y = \frac{\partial\omega}{\partial l} = 2\mu^2 k\bar{q}_y l \Big/ \left\{r\cos\phi\left(\mu^2 l^2 + \frac{f^2}{N^2}\nu^2 m^2 + \frac{k^2}{r^2\cos^2\phi} + \frac{f^2}{4H^2N^2}\right)^2\right\}, \tag{3.5}$$

$$C_{(g)}{}^Z = \frac{\partial\omega}{\partial m} = 2\nu^2 k\bar{q}_y m f^2 \Big/ \left\{r\cos\phi N^2 \times \left(\mu^2 l^2 + \frac{f^2}{N^2}\nu^2 m^2 + \frac{k^2}{r^2\cos^2\phi} + \frac{f^2}{4H^2N^2}\right)^2\right\} \tag{3.6}$$

(see, for example, Whitham, 1974). These expressions may be simplified by using the equality

$$f^2\overline{q'^2_{(M)}} = \tfrac{1}{2}e^{z/H}|\psi|^2\left(\mu^2 l^2 + \frac{f^2}{N^2}\nu^2 m^2 + \frac{k^2}{r^2\cos^2\phi} + \frac{f^2}{4H^2N^2}\right)^2.$$

Now since $\mu l = \zeta_y$, $\nu m = \zeta_z$, then from (2.8)

$$A_{(M)} = \frac{1}{4}\frac{r\cos\phi|\psi|^2}{\bar{q}_y f^2}\left\{(\zeta_y)^2 + \frac{f^2}{N^2}(\zeta_z)^2 + \frac{k^2}{r^2\cos^2\phi} + \frac{f^2}{4H^2N^2}\right\}^2, \tag{3.7}$$

$$C_{(g)}{}^Y = \frac{k|\psi|^2}{2f^2A_{(M)}}\mu\zeta_y ,$$

$$C_{(g)}{}^Z = \frac{k|\psi|^2}{2N^2A_{(M)}}\nu\zeta_z .$$

Hence, defining the pair $(C_{(g)}{}^Y, C_{(g)}{}^Z)$ to transform as a vector under a general coordinate transformation in the meridional plane, so that

$$C_{(g)}{}^y = \frac{dy}{dY}C_{(g)}{}^Y,$$

$$C_{(g)}{}^z = \frac{dz}{dZ}C_{(g)}{}^Z,$$

then the group velocity in (y, z) coordinates can be written as

$$C_g{}^y = \frac{k|\psi|^2}{2f^2A_{(M)}}\zeta_y , \tag{3.8}$$

$$C_g{}^z = \frac{k|\psi|^2}{2N^2A_{(M)}}\zeta_z . \tag{3.9}$$

Finally, writing (2.2) in terms of $|\psi|$ and ζ,

$$\mathbf{F} = \tfrac{1}{2}k|\psi|^2\left(\frac{1}{f^2}\zeta_y, \frac{1}{N^2}\zeta_z\right) \tag{3.10}$$

(a result which does not require ζ to have a locally-plane wave form). Hence combining (3.8)–(3.10),

$$\mathbf{F} = A_{(M)}\mathbf{C}_{(g)} . \tag{3.11}$$

If the EP flux is defined to transform as a vector from (y, z) coordinates to any other coordinate system, then (3.11) is a manifestly coordinate invariant result, and F is always parallel to $\mathbf{C}_{(g)}$. Furthermore, from (2.9), $\mathbf{C}_{(M)} = \mathbf{C}_{(g)}$ in the WKBJ limit.

From (3.7), (3.8) and (3.9), $A_{(M)}$, $C_{(g)}{}^y$ and $C_{(g)}{}^z$ do not depend on μ and ν. Hence, within the WKBJ approximation, the EP flux is also parallel to the group velocity derived from the eddy potential vorticity equation

$$\left(\frac{\partial}{\partial t} + \bar{u}\frac{\partial}{\partial x}\right)q' + \bar{q}_y v' = 0.$$

For WKBJ theory to apply, the phase function ζ must vary rapidly in space compared with any factor connected with the sphericity of the earth. On the other hand, for planetary-scale waves, the slowly varying functions ζ_y, ζ_z and $|\psi|$ will, by definition, have comparable variation with such spherical factors.

4. EP flux and refractive index

For simplicity consider a stationary wave so that the dispersion relation (3.4) can be written in the form

$$(\zeta_y)^2 + \frac{f^2}{N^2}(\zeta_z)^2 = \frac{Q}{r^2}, \tag{4.1}$$

where

$$Q = r^2\bar{q}_y/\bar{u} - k^2/\cos^2\phi - f^2r^2/4H^2N^2,$$

is Matsuno's refractive index squared. Now there is a unique coordinate system $(\tilde{y}, \tilde{z})$ in which (4.1) is essentially isotropic in horizontal and vertical derivatives. This is given by the transformation

$$d\tilde{y} = \frac{f}{\Omega}dy,$$

$$d\tilde{z} = \frac{N}{\Omega}dz,$$

whence (4.1) becomes

$$(\zeta_{\tilde{y}})^2 + (\zeta_{\tilde{z}})^2 = \tilde{Q}/4r^2, \tag{4.2}$$

where

$$\tilde{Q} = Q/\sin^2\phi.$$

It is important to note that the requirement that $d\tilde{y}$ and $d\tilde{z}$ be exact differentials, a property which will be used below, uniquely fixes this isotropic coordinate system. Notice also that each term in (4.2) is slowly varying, i.e., has variation comparable with the earth's sphericity.

The form (4.2) of the dispersion relation gives rise to a simple yet exact relation between the curvature of the integral curves of the EP flux (or EP flux trajectories) and the gradient of $\tilde{Q}$. This has been discussed briefly in Palmer (1981b) and used as a model diagnostic by Butchart *et al.* (1982); however, in view of the importance of this relation it is worthwhile giving a more extensive account here, emphasizing in particular the difficulty in expressing this result in a coordinate invariant form.

Differentiating (4.2) with respect to $\tilde{y}$ and $\tilde{z}$ gives

$$\zeta_{\tilde{y}}\zeta_{\tilde{y}\tilde{y}} + \zeta_{\tilde{z}}\zeta_{\tilde{z}\tilde{y}} = \frac{1}{8r^2}\tilde{Q}_{\tilde{y}} , \tag{4.3}$$

$$\zeta_{\tilde{y}}\zeta_{\tilde{y}\tilde{z}} + \zeta_{\tilde{z}}\zeta_{\tilde{z}\tilde{z}} = \frac{1}{8r^2}\tilde{Q}_{\tilde{z}} . \tag{4.4}$$

Now defining a vector whose components in $(\tilde{y}, \tilde{z})$ coordinates are

$$\mathbf{P} = (\zeta_{\tilde{y}}, \zeta_{\tilde{z}}),$$

then using the identity

$$\zeta_{\tilde{y}\tilde{z}} = \zeta_{\tilde{z}\tilde{y}} ,$$

(which, of course, only holds if $d\tilde{y}$ and $d\tilde{z}$ are exact differentials), (4.3) and (4.4) can be written as

$$(\mathbf{P}\cdot\nabla)\mathbf{P} = \frac{1}{8r^2}\nabla\tilde{Q}, \tag{4.5}$$

where ∇ stands for the gradient operator $(\partial/\partial\tilde{y}, \partial/\partial\tilde{z})$.

Now, since we have defined the EP flux to transform as a vector, its components in the $(\tilde{y}, \tilde{z})$ coordinate system are given by

$$F^{\tilde{y}} = \frac{d\tilde{y}}{dy}F^y = \frac{1}{2\Omega^2}k|\psi|^2\zeta_y , \tag{4.6}$$

$$F^{\tilde{z}} = \frac{d\tilde{z}}{dz}F^z = \frac{1}{2\Omega^2}k|\psi|^2\zeta_z . \tag{4.7}$$

Hence, in the $(\tilde{y}, \tilde{z})$ coordinate system (and therefore in all coordinate systems),

$$\mathbf{F} = \frac{1}{2\Omega^2}k|\psi|^2\mathbf{P},$$

and F is parallel to P.

Now the integral curves $\mathbf{x}(t)$ of P (and therefore F) are, by definition, solutions of the equation

$$\mathbf{P} = d\mathbf{x}(t)/dt \tag{4.8}$$

for some parameter t along the integral curves. Substituting (4.8) into (4.5) we have

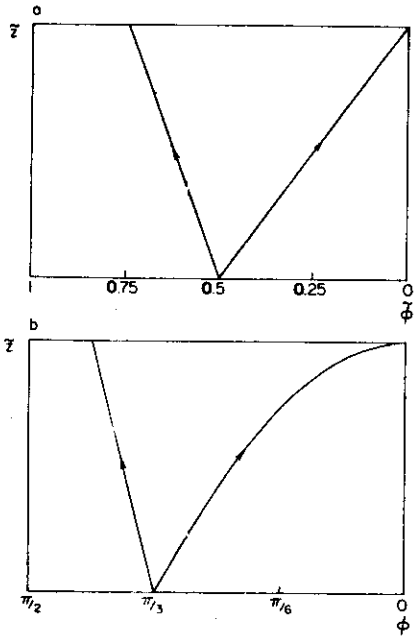

FIG. 1. (a) Two (hypothetical) EP flux trajectories on a $(\tilde{\phi}, \tilde{z})$ grid, where $\tilde{\phi} = (1 - \cos\phi)$ (so that $d\tilde{\phi} = \sin\phi d\phi$). Since the trajectories are straight the refractive index gradient is zero. (b) The same trajectories in $(\phi, \tilde{z})$ coordinates. There is no refraction, yet the trajectories are curved.

$$\frac{d^2\mathbf{x}(t)}{dt^2} = \frac{1}{8r^2}\nabla\tilde{Q}.$$

This equation shows that $\tilde{Q}$ acts as a potential function, curving the trajectories $\mathbf{x}(t)$ up its gradient.

Another way of seeing the role of $\tilde{Q}$ as a potential function is to consider the angle Θ that the EP flux (or $\mathbf{P}$, or $\mathbf{C}_{(\phi)}$) makes with the horizontal in the $(\tilde{y}, \tilde{z})$ coordinate system. From (4.6) and (4.7)

$$\tan\Theta = \zeta_z/\zeta_y.$$

The rate of change of Θ with respect to the parameter t is given by

$$\sec^2\Theta\frac{d\Theta}{dt} = \left(\frac{d\zeta_z}{dt}\zeta_y - \frac{d\zeta_y}{dt}\zeta_z\right)\Big/(\zeta_y)^2,$$

which, rearranging and using (4.5) becomes

$$\frac{d\Theta}{dt} = \frac{1}{(\zeta_y)^2 + (\zeta_z)^2}[\tilde{Q}_z\zeta_y - \tilde{Q}_y\zeta_z]\frac{1}{8r^2}. \quad (4.9)$$

If we write

$$\nabla\tilde{Q} = \mathbf{i}(\nabla\tilde{Q})^{\parallel} + \mathbf{j}(\nabla\tilde{Q})^{\perp},$$

where $\mathbf{i}$ and $\mathbf{j}$ are unit vectors parallel and perpendicular to $\mathbf{P}$ respectively, then (4.9) can be written as

$$\left|\frac{d\Theta}{dt}\right| = \frac{|(\nabla\tilde{Q})^{\perp}|}{8\|\mathbf{P}\|r^2}, \quad (4.10)$$

where

$$\|\mathbf{P}\|^2 = (\zeta_y)^2 + (\zeta_z)^2.$$

Eq. (4.10) makes it clear that the integral curves of $\mathbf{F}$, $\mathbf{P}$, or $\mathbf{C}_{(\phi)}$ are refracted by the component of the gradient of $\tilde{Q}$ normal to these curves. For comparison, the form of refractive index used by Karoly and Hoskins (1982) is equal to $Q\cos^2\phi$, and the form used by O'Neill and Youngblut (1982) is essentially equal to Q. Both of these forms are only approximate for planetary-scale motions. For example, Karoly and Hoskins define a Mercator coordinate y^* such that $dy^* = \sec\phi\, dy$, and a vertical coordinate z^* such that $dz^* = N\sec\phi/f dz$. In terms of (y^*, z^*), (4.1) becomes

$$(\zeta_{y^*})^2 + (\zeta_{z^*})^2 = Q\cos^2\phi/r^2.$$

However, the analysis following (4.1) fails if it is applied to the above equation because

$$\zeta_{y^*z^*} \neq \zeta_{z^*y^*},$$

i.e., dz^* is not an exact differential [alternatively, there is no function $z^*(y, z)$ satisfying $dz^* = N\sec\phi/f dz$]. The effect of allowing full variation of f is illustrated in Fig. 2 of Karoly and Hoskins (1982). Reference to that figure shows that ray paths calculated using full variation of f are more strongly refracted in low latitudes than if f is held at a constant midlatitude value. This is consistent with the rapid growth of $1/\sin^2\phi$ as $\phi \to 0$. One practical consequence of the singularity of $1/\sin^2\phi$ at $\phi = 0$ is that when refractive index theory is appropriate, EP fluxes should have little or no vertical component in low latitudes, irrespective of the position of the subtropical zero wind line, i.e., irrespective of whether Q itself becomes large in the tropics. This appears to be borne out by observation (Palmer, 1981a). Hence the dynamics embodied in the governing equations require that in the tropics the meridional heat flux of forced planetary waves should be very small.

The equations (4.5) and (4.10) only strictly hold in the $(\tilde{y}, \tilde{z})$ coordinate system. In practice, however, EP fluxes are plotted on a standard latitude–height grid (usually scaled by f_0^2/N_0^2, where N_0^2 is a typical value of N). With this grid EP flux trajectories may be curved both because the refractive index gradient is non-zero, and, independently, because of the distortion of the grid relative to $(\tilde{y}, \tilde{z})$ coordinates. In the stratosphere, where the Brunt-Vaisalla frequency

is nearly constant, this variation is due almost entirely to the effect of the variation of the Coriolis parameter.

Fig. 1 illustrates the effect of this coordinate distortion. We assume that N^2 is constant so that the vertical scales in Fig. 1a and b are identical (and arbitrary). Fig. 1a shows two hypothetical EP flux trajectories under (unlikely) circumstances where the gradient of $\tilde{Q}$ is zero. Fig. 1b shows how this trajectory looks curved on a regular latitude–height diagram, even though there is no refraction. In high latitudes this curvature is not noticeable; south of ~45°N it becomes more noticeable. In practice, however, variations in the low-latitude refractive index (see above) would generally be dominant over the effects of this coordinate distortion.

The technical reason that the curvature of EP flux trajectories is coordinate-dependent is that in (4.5) the quantity $(\mathbf{P}\cdot\nabla)\mathbf{P}$ does not transform as a vector so that (4.5) is not, as written, a coordinate invariant equation. The machinery necessary to describe the law of refraction of the EP flux, or group velocity, in a manifestly coordinate invariant manner is well known in other branches of physics (see, for example, Sommerfeld, 1964) requiring the use of affine connection coefficients and the associated covariant derivative.

Acknowledgments. My thanks to Dr. A. O'Neill for many helpful discussions, and Dr. N. Butchart for correspondence. This research was supported by the National Aeronautics and Space Administration Grant NAG2-66.

REFERENCES

Burger, A. P., 1958: Scale consideration of planetary motions of the atmosphere. *Tellus*, **10**, 195–205.

Butchart, N., S. A. Clough, T. N. Palmer and P. J. Trevelyan, 1982: Simulations of an observed stratospheric warming with quasigeostrophic refractive index as a model diagnostic. *Quart. J. Roy. Meteor. Soc.*, **108** (in press).

Dunkerton, T., C.-P. Hus and M. E. McIntyre, 1981: Some Eulerian and Lagrangian diagnostics for a model stratospheric warming. *J. Atmos. Sci.*, **38**, 819–843.

Edmon, H. J., B. J. Hoskins and M. E. McIntyre, 1980: Eliassen-Palm cross-sections for the troposphere. *J. Atmos. Sci.*, **37**, 2600–2616 (see also Corrigendum, *J. Atmos. Sci.*, **38**, 1115, especially second last item).

Karoly, D. J., and B. J. Hoskins, 1982: Three dimensional propagation of planetary waves. *J. Meteor. Soc. Japan*, Centennial Issue (in press).

Lorenz, E. N., 1960: Energy and numerical weather prediction. *Tellus*, **12**, 364–373.

Matsuno, T., 1970: Vertical propagation of stationary planetary waves in the winter Northern Hemisphere. *J. Atmos. Sci.*, **27**, 871–883.

——, 1971: A dynamical model of the stratospheric sudden warming. *J. Atmos. Sci.*, **28**, 1479–1494.

O'Neill, A., and C. E. Youngblut, 1982: Stratospheric warmings diagnosed using the transformed Eulerian-mean equations and the effect of the mean state on wave propagation. *J. Atmos. Sci.*, **39** (in press).

Palmer, T. N., 1981a: Diagnostic study of a wavenumber-2 stratospheric sudden warming in a transformed Eulerian-mean formalism. *J. Atmos. Sci.*, **38**, 844–855.

——, 1981b: Aspects of stratospheric sudden warmings studied from a transformed Eulerian-mean viewpoint. *J. Geophys. Res.*, **86**, 9679–9687.

Sommerfeld, A., 1964: *Mechanics of Deformable Bodies*. Academic Press, pp. 396.

Whitham, G. B., 1974: *Linear and Nonlinear Waves*. Wiley, pp. 636.